

Central schemes for systems of non-local balance laws

Sanjibanees Sudha*, Jan Friedrich† and Samala Rathan*

January 27, 2025

Abstract

We present numerical approaches to approximate the solutions of systems of non-local balance laws. In particular, we derive a non-staggered central scheme based on the well-known Nessyahu-Tadmor scheme and show that it preserves the positivity of solutions. To reduce the numerical diffusion, we then consider a non-local version of the Kurganov-Tadmor scheme. For both schemes, an appropriate approximation of the non-local term is crucial to maintain a second-order accuracy. Numerical examples validate our theory and demonstrate its applicability to various systems of non-local problems.

Keywords: System of non-local balance laws, higher-order schemes, finite-volume schemes, central schemes, non-staggered grid, traffic flow

1 Introduction

Systems of balance laws are of great importance in the modeling and comprehension of complex physical phenomena, as they are capable of describing the interaction of multiple quantities that evolve over time. In recent years, there has been a growing interest in non-local extensions of well-known hyperbolic balance laws, e.g. [1, 2, 3, 5, 9, 10, 11, 13, 14, 22, 24, 29, 32, 34] and the references therein. We also refer to [33] for an overview on recent results. Similar to [1], a generalized form of a system of N non-local balance laws in one spatial dimension can be expressed as follows

$$\partial_t \boldsymbol{\rho}(t, x) + \partial_x F(\boldsymbol{\rho}, \omega * \boldsymbol{\rho}) = S(\boldsymbol{\rho}, \omega * \boldsymbol{\rho}), \quad (1.1)$$

$$\boldsymbol{\rho}(t, 0) = \boldsymbol{\rho}_0(x), \quad (1.2)$$

with $t \in \mathbb{R}_+$, $x \in \mathbb{R}$, $\boldsymbol{\rho}(t, x) \in \mathbb{R}^N$, $\omega : \mathbb{R} \rightarrow \mathbb{R}^{m \times N}$, $(\omega * \boldsymbol{\rho})(t, x) \in \mathbb{R}^m$, $F : \mathbb{R}^N \times \mathbb{R}^m \rightarrow \mathbb{R}^N$, $S : \mathbb{R}^N \times \mathbb{R}^m \rightarrow \mathbb{R}^N$, suitable initial data $\boldsymbol{\rho}_0 : \mathbb{R} \rightarrow \mathbb{R}^N$, and where the non-local term $\omega * \boldsymbol{\rho}$, for $\ell = 1, \dots, m$ is given by,

$$(\omega * \boldsymbol{\rho})_\ell(t, x) = \sum_{k=1}^N \underbrace{\int_{\mathbb{R}} \omega^{\ell, k}(x - y) \rho^k(t, y) dy}_{=: R^{\ell, k}(t, x)}.$$

Here we use boldface variables for vector expressions and to shorten the notation we use $\mathbf{R}(t, x) = (\omega * \boldsymbol{\rho})(t, x)$. We assume that each kernel $\omega^{\ell, k} : \mathbb{R} \rightarrow \mathbb{R}_+$ is of compact support

†RWTH Aachen University, Institute of Applied Mathematics, 52064 Aachen, Germany (friedrich@igpm.rwth-aachen.de)

*Department of Humanities and Sciences, Indian Institute of Petroleum and Energy, Visakhapatnam, Andhra Pradesh, India-530003 ({sudhamath21, rathans.math}@iipe.ac.in)

centered around zero, i.e., the support of each kernel is given by the interval $[\eta_1^{\ell,k}, \eta_2^{\ell,k}]$ with $\eta_1^{\ell,k} \leq 0 \leq \eta_2^{\ell,k}$, $\eta_1^{\ell,k} \neq \eta_2^{\ell,k}$, for $k = 1, \dots, N$ and $\ell = 1, \dots, m$. It should be noted that the proof of existence and uniqueness for equation (1.1) is not yet complete, and as in the local case, it is a challenging task. Nevertheless, for the case of a system of non-local conservation laws and a coupling of those solely through the non-local term, rather general results can be found in [1, 2] and results for specific flux functions in [5, 10, 13, 22]. Similar, to the local setting the scalar case $N = 1$ is well understood, see e.g. [4, 14, 32].

Especially in the scalar case, many applications can be modeled by (1.1), such as sedimentation processes [9], granular material dynamics [3], supply chains [18, 20], material flow on a conveyor belt (two spatial dimensions) [29], crowd dynamics (two spatial dimensions) [17, 18], and particularly traffic flows [11, 14, 24]. Examples of systems with a non-local term in the flux as in (1.1) include traffic flow models with a second equation describing the momentum [13], multiclass models [15], or multilane models [5, 22], multi-population crowd dynamics [19], a non-local extension of the Keyfitz-Kranzer model [1, 2], or more recently, pressureless and non-local Euler equations with relaxation [10].

Numerical schemes for non-local conservations are typically based on ideas for schemes used to approximate local hyperbolic balance laws. Especially for the scalar case, first-order methods are reliable, robust and well understood, see e.g. [4, 14, 25, 30]. Similar to the local schemes, finite-volume methods are considered, in particular Godunov-type schemes (upwind method) [28], and Lax-Friedrichs schemes (LxF) (central scheme) are widely used for non-local conservation laws. Note that in contrast to the local setting no Riemann solvers are known, but for certain structures of the flux Godunov/upwind-type schemes can still be derived, e.g. [24, 25]. Central schemes avoid this by integrating over space-time control volumes where each Riemann fan is contained within its own volume. This results in a more dissipative behavior, but their advantage is the simplicity and direct applicability to different flux functions, such as those given by the system (1.1). In contrast, Godunov methods are quite difficult to derive for (1.1). However, for special structures of the flux (e.g. a coupling only through the non-local term) they can be derived in a straightforward way [2, 15, 22].

Apart from first-order schemes, higher-order schemes for non-local scalar conservation laws have been developed in [12, 23, 41]. In [38], the authors considered the case for systems with second-order MUSCL-type interpolants with underlined LxF flux and proved positivity preserving property when coupled with Runge-Kutta time integration schemes. All these works consider a higher-order reconstruction within each cell and an appropriate flux function at the cell interface. Furthermore, high-resolution schemes based on the ideas of central schemes have been considered in [6, 7, 26, 35]. These ideas go back to the central differencing high resolution scheme developed by Nessyahu and Tadmor in [39]. To reduce the dissipative behavior of first order central schemes they used MUSCL-type interpolants and maintained the simplicity of the Riemann-solver free approach by evolving the cell-averages over staggered cells. The resulting and so-called central Nessyahu-Tadmor (NT) scheme is a second-order accurate method. The staggered grids can also be transformed into a non-staggered grid by following [31]. The main property of non-staggered schemes is the further simplicity since they avoid the need to alternate between two staggered grids, which is particularly challenging near the boundaries. The major drawback of these central schemes is their relatively large numerical dissipation. To further reduce the numerical dissipation, modifications of the NT scheme were proposed in [36] by further splitting cells into smooth and non-smooth parts and treating them differently, resulting in the so-called Kurganov-Tadmor (KT) scheme which is still second-order accurate. In [35] the latter scheme was investigated for a specific non-local traffic flow model.

The aim of this work is to develop high-resolution central schemes using non-staggered grids for a general non-local system such as (1.1). Therefore, in section 2, we extend the NT

schemes considered in [6, 26] to systems of non-local balance laws and use the ideas of [31] to consider them on a non-staggered grid. In addition, we prove that the NT schemes satisfies similar bounds as the analytic equation. In particular, the positivity is preserved. To reduce the numerical diffusion, we extend the approach in [36] to the non-local setting, see section 3. Finally, in section 4, we present several numerical examples that demonstrate the second-order accuracy of the considered schemes and their applicability to various modeling equations.

2 Non-staggered central scheme

In the following we assume that the system (1.1) is only coupled through the non-local term or the source, i.e., for $k = 1, \dots, N$ we have

$$\partial_t \rho^k(t, x) + \partial_x F_k(\rho^k, \omega * \rho) = S_k(\rho, \omega * \rho). \quad (2.1)$$

In addition, we assume $F_k \in C^2(\mathbb{R} \times \mathbb{R}^m; \mathbb{R})$ and $\partial_\rho F_k \in L^\infty(\mathbb{R} \times \mathbb{R}^m; \mathbb{R})$ for every $k = 1, \dots, N$.

Remark 2.1. We note that the derivation below can also be applied to the balance law (1.1), but it is more challenging to derive a CFL condition. Nevertheless, several relevant applications can already be modeled by (2.1), see also Section 4. Therefore our focus is on deriving second-order schemes to solve (2.1) instead of proving the well-posedness. In particular, many models contain source terms and kernels with compact support, which need to be approximated appropriately. For a zero source term and more regular kernels, the existence and uniqueness of weak entropy solutions of (2.1) is guaranteed by the analysis done in [1] (under additional assumptions on F).

2.1 Non-staggered Nessyahu-Tadmor scheme

To derive approximate solutions to (1.1) we discretize space and time by an equidistant grid, where Δx is the step size in space and Δt is the step size in time. So, $t^n = n\Delta t$ with $n \in \mathbb{N}$ is the time grid and $x_j = j\Delta x$ with $j \in \mathbb{Z}$ the space grid. The cell interfaces are $x_{j-1/2}$ and $x_{j+1/2}$. For simplicity, we assume that the size of the space step Δx can be chosen such that for $\ell = 1, \dots, m$ and $k = 1, \dots, N$ every $N_1^{\ell, k} := |\eta_1^{\ell, k}|/\Delta x$ and $N_2^{\ell, k} := \eta_2^{\ell, k}/\Delta x$ are natural numbers or zero.

Remark 2.2. We note that for the case where all kernels have the same support and are either solely forward/backward oriented or symmetric, the previous assumption holds. Otherwise, we need to set $N_1^{\ell, k} := \lceil |\eta_1^{\ell, k}|/\Delta x \rceil$ and $N_2^{\ell, k} := \lceil \eta_2^{\ell, k}/\Delta x \rceil$. This results in minor modifications when computing the non-local terms, which are detailed below.

The initial data (1.2) are approximated component-wise for $k = 1, \dots, N$ and $j \in \mathbb{Z}$ by

$$\rho_j^{k, 0} = \frac{1}{\Delta x} \int_{x_{j-1/2}}^{x_{j+1/2}} \rho_0^k(x) dx.$$

We assume that the cell-averages of the solution are given at a time t^n by

$$\rho_j^k(t) = \frac{1}{\Delta x} \int_{x_{j-1/2}}^{x_{j+1/2}} \rho^k(t^n, x) dx.$$

To evolve the cell-averages to the next time level t^{n+1} , we start by reconstructing a piecewise linear function in each cell, component-wise for $k = 1, \dots, N$ by

$$\tilde{\rho}_j^k(t, x) = \rho_j^k(t) + s_j^k(x - x_j) \text{ for } x \in [x_{j-1/2}, x_{j+1/2}). \quad (2.2)$$

One way to compute the derivative in each component is to use the minmod limiter

$$s_j^k = \text{minmod} \left(\frac{\rho_j^k(t) - \rho_{j-1}^k(t)}{\Delta x}, \frac{\rho_{j+1}^k(t) - \rho_j^k(t)}{\Delta x} \right), \quad (2.3)$$

where the minmod function is defined as

$$\text{minmod}(a, b) = \begin{cases} a, & \text{if } |a| < |b| \text{ and } a \cdot b > 0, \\ b, & \text{if } |b| < |a| \text{ and } a \cdot b > 0, \\ 0, & \text{if } a \cdot b \leq 0. \end{cases} \quad (2.4)$$

The reconstruction (2.2) preserves the conservation (here the cell-average $\rho_j^k(t)$ in $[x_j, x_{j+1}]$). Next, we evolve the cell-averages with the help of the piecewise linear reconstruction (2.2) by integrating (1.1) over the domain $[t^n, t^{n+1}] \times [x_j, x_{j+1})$ for each $k = 1, \dots, N$,

$$\begin{aligned} \rho_{j+1/2}^{k,n+1} &= \frac{1}{\Delta x} \int_{x_j}^{x_{j+1}} \tilde{\rho}^k(t^n, x) dx - \frac{1}{\Delta x} \int_{t^n}^{t^{n+1}} F_k(\rho_{j+1}^k(t), \mathbf{R}(t, x_{j+1})) - F_k(\rho_j^k(t), \mathbf{R}(t, x_j)) dt \\ &\quad + \frac{1}{\Delta x} \int_{t^n}^{t^{n+1}} \int_{x_j}^{x_{j+1}} S_k(\tilde{\rho}_j(t, x), \mathbf{R}(t, x)) dx dt, \\ &= \frac{1}{\Delta x} \left(\int_{x_j}^{x_{j+1/2}} \tilde{\rho}_j^k(t^n, x) dx + \int_{x_{j+1/2}}^{x_{j+1}} \tilde{\rho}_{j+1}^k(t^n, x) dx \right) - \frac{1}{\Delta x} \left(\int_{t^n}^{t^{n+1}} F_k(\rho_{j+1}^k(t), \mathbf{R}(t, x_{j+1})) \right. \\ &\quad \left. - F_k(\rho_j^k(t), \mathbf{R}(t, x_j)) \right) dt + \frac{1}{2} \left(\int_{t^n}^{t^{n+1}} S_k(\rho_{j+1}(t), \mathbf{R}(t, x_{j+1})) + S_k(\rho_j(t), \mathbf{R}(t, x_j)) dt \right). \end{aligned}$$

Due to the finite speed of propagation we introduce the CFL condition similar to [6, 27]

$$\Delta t \leq \frac{\Delta x}{2\lambda_{\max}} \quad \text{with} \quad \lambda_{\max} = \max_{k=1, \dots, N} \|\partial_\rho F_k\|_{L^\infty(\mathbb{R} \times \mathbb{R}^m; \mathbb{R})}. \quad (2.5)$$

This allows us to use the mid point-rule for the flux term.

$$\begin{aligned} \rho_{j+1/2}^{k,n+1} &= \frac{1}{2}(\rho_j^{k,n} + \rho_{j+1}^{k,n}) + \frac{\Delta x}{8}(s_j^{k,n} - s_{j+1}^{k,n}) - \frac{\Delta t}{\Delta x} \left[F_k(\rho_{j+1}^{k,n+1/2}, \mathbf{R}_{j+1}^{n+1/2}) - F_k(\rho_j^{k,n+1/2}, \mathbf{R}_j^{n+1/2}) \right] \\ &\quad + \frac{\Delta t}{2} \left[S_k(\rho_{j+1}^{n+1/2}, \mathbf{R}_{j+1}^{n+1/2}) + S_k(\rho_j^{n+1/2}, \mathbf{R}_j^{n+1/2}) \right]. \end{aligned} \quad (2.6)$$

To approximate the source term accurately we used the trapezoidal rule in space and the mid-point rule in time. In particular, the source and flux terms use the same input, which avoids additional computational effort. It remains to approximate the values at the time $t^{n+1/2}$. Thanks to a Taylor series expansion and the balance law (1.1), we have

$$\rho_j^{k,n+1/2} \approx \rho^k(t^n, x_j) + \frac{\Delta t}{2} \rho_t^k(t^n, x_j) \approx \rho_j^{k,n} + \frac{\Delta t}{2} S_k(\rho_j^n, \mathbf{R}_j^n) - \frac{\Delta t}{2} \sigma^k(\rho_j^n, \mathbf{R}_j^n), \quad (2.7)$$

$$\sigma^k(\rho_j^n, \mathbf{R}_j^n) = \text{minmod} \left(\frac{F_k(\rho_j^{k,n}, \mathbf{R}_j^n) - F_k(\rho_{j-1}^{k,n}, \mathbf{R}_{j-1}^n)}{\Delta x}, \frac{F_k(\rho_{j+1}^{k,n}, \mathbf{R}_{j+1}^n) - F_k(\rho_j^{k,n}, \mathbf{R}_j^n)}{\Delta x} \right). \quad (2.8)$$

Note that for the non-local term $\mathbf{R}(t, x)$ we have that each element is given by

$$R^\ell(t, x) = \sum_{k=1}^N R^{\ell,k}(t, x).$$

Hence, we need to approximate $R^{\ell,k}(t^{n+1/2}, x_j)$. To simplify the notation we will neglect the indices $\ell = 1, \dots, m$ in the following lines. This can also be viewed as considering the special case $m = 1$. As before we use a Taylor expansion

$$R_j^{k,n+1/2} \approx R_j^{k,n} + \frac{\Delta t}{2} R_t^k(t^n, x_j). \quad (2.9)$$

We approximate the convolution term using the midpoint rule,

$$\begin{aligned} R^k(t^n, x_j) &= \int_{x_{j-N_1^k}}^{x_{j+1/2-N_1^k}} \tilde{\rho}^k(t^n, y) \omega^k(y - x_j) dy + \sum_{l=-N_1^k}^{N_2^k-2} \int_{x_{j+1/2+l}}^{x_{j+3/2+l}} \tilde{\rho}^k(t^n, y) \omega^k(y - x_j) dy \\ &\quad + \int_{x_{j+N_2^k-1/2}}^{x_{j+N_2^k}} \tilde{\rho}^k(t^n, x) \omega^k(y - x_j) dy, \\ &= \frac{\Delta x}{2} \left(\rho_{j-N_1^k}^{k,n} + \frac{\Delta x}{4} s_{j-N_1^k}^{k,n} \right) \omega^k \left(\frac{\Delta x}{4} - N_1^k \Delta x \right) + \Delta x \sum_{l=-N_1^k}^{N_2^k-2} \rho_{j+l+1}^{k,n} \omega^k((l+1)\Delta x) \\ &\quad + \frac{\Delta x}{2} \left(\rho_{j+N_2^k}^{k,n} - \frac{\Delta x}{4} s_{j+N_2^k}^{k,n} \right) \omega^k \left(N_2^k \Delta x - \frac{\Delta x}{4} \right). \end{aligned} \quad (2.10)$$

To calculate R_t we use again an appropriate quadrature rule and the balance law (1.1)

$$\begin{aligned} R_t^k(t^n, x_j) &\approx \frac{\Delta x}{2} \left(S_k(\rho_{j-N_1^k}^n, \mathbf{R}_{j-N_1^k}^n) - \sigma^k(\rho_{j-N_1^k}^n, \mathbf{R}_{j-N_1^k}^n) \right) \omega^k \left(\frac{\Delta x}{4} - N_1^k \Delta x \right) \\ &\quad + \Delta x \sum_{l=-N_1^k}^{N_2^k-2} \left(S_k(\rho_{j+l+1}^n, \mathbf{R}_{j+l+1}^n) - \sigma^k(\rho_{j+l+1}^n, \mathbf{R}_{j+l+1}^n) \right) \omega^k((l+1)\Delta x) \\ &\quad + \frac{\Delta x}{2} \left(S_k(\rho_{j+N_2^k}^n, \mathbf{R}_{j+N_2^k}^n) - \sigma^k(\rho_{j+N_2^k}^n, \mathbf{R}_{j+N_2^k}^n) \right) \omega^k \left(N_2^k \Delta x - \frac{\Delta x}{4} \right). \end{aligned} \quad (2.11)$$

The space derivative of the flux is approximated as before by the minmod limiter, i.e., equation (2.8).

Let us make the following remarks to the approximation of the non-local terms in (2.10) and (2.11):

Remark 2.3. We note that the first and last interval in (2.11) are approximated by the following first order quadrature rule

$$\int_a^b f(x)g(x)dx \approx (b-a)f(a)g\left(\frac{a+b}{2}\right).$$

On the one hand, a first order approximation of $R_t^k(t^n, x_j)$ is sufficient to maintain the second order accuracy of $R_j^{k,n+1/2}$. On the other hand, this specific quadrature rule allows us to use the same weights as in (2.10) and it does not involve any additional (spatial) evaluations of the source term or the slopes, such that we can rely on already computed values in the implementation.

Remark 2.4. In contrast to previous works as [6, 27], we approximate the time derivative of the non-local term by using the minmod limiter. Since the slopes are already used to compute (2.7), this approach is rather simple. Alternatively, one can proceed by applying integration by parts as in [6, 27] which requires the derivative of the kernel ω .

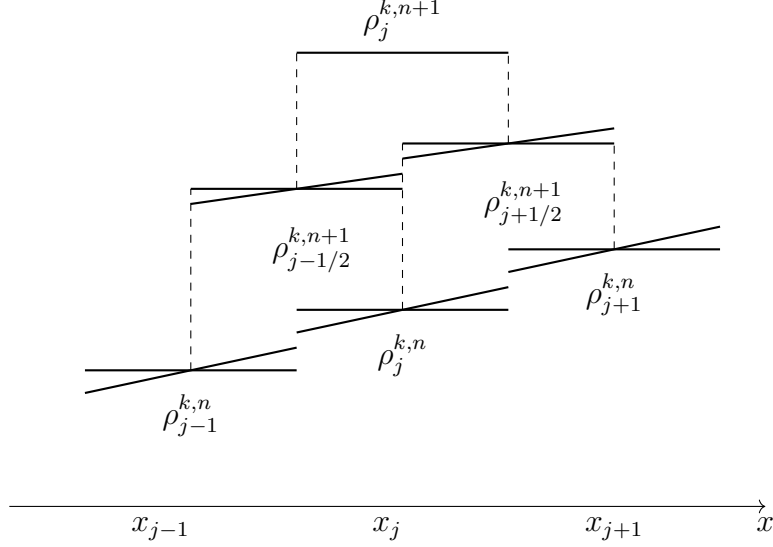


Figure 1: NT scheme reconstruction from non-staggered to staggered grid for fixed $k \in \{1, \dots, N\}$, compare Figure 3.1 from [31]

Remark 2.5. In case it is not possible to choose a grid such that all $|\eta_1^k|/\Delta x$ and $\eta_2^k/\Delta x$ are natural numbers, the first and last intervals for the approximation of the integrals need to be changed. Instead of computing a second-order accurate approximation over the intervals $[x_{j-N_1^k}, x_{j-N_1^k+1/2}]$ and $[x_{j+N_2^k-1/2}, x_{j+N_2^k}]$ in (2.10), we compute it for $[x_j + \eta_1^k, x_{j-N_1^k+1/2}]$ and $[x_{j+N_2^k-1/2}, x_j + \eta_2^k]$.

Now, we convert the staggered second-order scheme (2.6)–(2.7) to non-staggered grid following [31]. First, reconstruct a piecewise-linear interpolant through the calculated staggered cell-averages at time t^{n+1} (see Figure 1) which is, for each $k = 1, \dots, N$, given by

$$\hat{\rho}_{j+1/2}^{k,n+1}(x) = \rho_{j+1/2}^{k,n+1} + s_{j+1/2}^{k,n+1}(x - x_{j+1/2}). \quad (2.12)$$

The staggered discrete derivatives, $s_{j+1/2}^{k,n+1}$, are given by

$$s_{j+1/2}^{k,n+1} = \text{minmod} \left(\frac{\Delta \rho_{j+1}^{k,n+1}}{\Delta x}, \frac{\Delta \rho_j^{k,n+1}}{\Delta x} \right), \quad (2.13)$$

with $\Delta \rho_j^{k,n+1} = \rho_{j+1/2}^{k,n+1} - \rho_{j-1/2}^{k,n+1}$. Then, the cell-averages at the next time step, ρ_j^{n+1} , are obtained by averaging the interpolant (2.12). This results in the following non-staggered corrector scheme for each $k = 1, \dots, N$

$$\begin{aligned} \rho_j^{k,n+1} &= \frac{1}{\Delta x} \left[\int_{x_{j-1/2}}^{x_j} \hat{\rho}_{j-1/2}^{k,n+1}(x) dx + \int_{x_j}^{x_{j+1/2}} \hat{\rho}_{j+1/2}^{k,n+1}(x) dx \right], \\ &= \frac{\rho_{j-1}^{k,n} + 2\rho_j^{k,n} + \rho_{j+1}^{k,n}}{4} - \frac{\Delta x}{16} (s_{j+1}^{k,n} - s_{j-1}^{k,n}) - \frac{\Delta x}{8} (s_{j+1/2}^{k,n+1} - s_{j-1/2}^{k,n+1}) \\ &\quad - \frac{\Delta t}{2\Delta x} \left[F_k(\rho_{j+1}^{k,n+1/2}, \mathbf{R}_{j+1}^{n+1/2}) - F_k(\rho_{j-1}^{k,n+1/2}, \mathbf{R}_{j-1}^{n+1/2}) \right] \\ &\quad + \frac{\Delta t}{4} \left[S_k(\rho_{j+1}^{n+1/2}, \mathbf{R}_{j+1}^{n+1/2}) + 2S_k(\rho_j^{n+1/2}, \mathbf{R}_j^{n+1/2}) + S_k(\rho_{j-1}^{n+1/2}, \mathbf{R}_{j-1}^{n+1/2}) \right]. \end{aligned} \quad (2.14)$$

Here, $s_j^{k,n+1}$ and $s_{j+1/2}^{k,n+1}$ are, respectively, the discrete derivatives at time levels t^n and t^{n+1} given in (2.3) and (2.13), and $\rho^{n+1/2}$ and $\mathbf{R}^{n+1/2}$ are predicted at time level $t^{n+1/2}$ according to (2.7) and (2.9), respectively.

2.2 Positivity-preserving property and L^∞ -estimate

We will now prove that under suitable assumptions on the modeling equations (2.1), the numerical approximations satisfies the bounds of the analytic solution.

Therefore, we follow [1] and assume in addition that for all $R \in \mathbb{R}^m$, $F_k(0, R) = 0$. Further, there exists an $M > 0$ such that for all $\rho \in \mathbb{R}$ and $R \in \mathbb{R}^m$, $\|\nabla_R F_k\| \leq M|\rho|$ and $\partial_\rho F_k \in W^{1,\infty}(\mathbb{R} \times \mathbb{R}^m; \mathbb{R})$. Here, $\|\cdot\|$ denotes the Euclidean norm. We also add more regularity to the kernel by assuming that is not only of compact support but also $\omega \in C^2 \cap W^{2,\infty}(\mathbb{R}; \mathbb{R}_+^{m \times N})$. Finally, we set the source terms to zero, i.e., $S_k(\boldsymbol{\rho}, R) = 0$ for all $\boldsymbol{\rho} \in \mathbb{R}^N$ and $R \in \mathbb{R}^m$. Then, we are in the setting of [1] (as a simplified one-dimensional case) and existence and uniqueness of solutions is guaranteed. In particular, solutions remain positive and are bounded from above by an exponential bound in time, compare [1, Theorem 2.3]. The NT scheme fulfills similar bounds:

Theorem 2.6. *For the initial datum $\boldsymbol{\rho}_0 \in L^\infty(\mathbb{R}; \mathbb{R}_+^N)$, the approximate solutions of the NT schemes (2.14) stay positive, i.e.,*

$$\rho_j^{k,n} \geq 0, \quad \text{for } j \in \mathbb{Z}, n \in \mathbb{N}, k \in \{1, \dots, N\},$$

under the CFL condition

$$\frac{\Delta t}{\Delta x} \lambda_{\max} \leq \kappa \leq \frac{\sqrt{2} - 1}{2}, \quad (2.15)$$

with λ_{\max} defined as in (2.5).

Proof. We prove the statement by induction. By the approximation of the initial data the statement is obvious for $n = 0$. For $k \in \{1, \dots, N\}$ and $n \in \mathbb{N}$ it is sufficient to prove the positivity of the approximations on the staggered grid $\rho_{j+1/2}^{k,n+1}$. Since $\rho_j^{k,n+1}$ is obtained by integrating over these approximations, its positivity follows.

We first consider the difference in the flux and add some zeros

$$\begin{aligned} & |F_k(\rho_{j+1}^{k,n+1/2}, \mathbf{R}_{j+1}^{n+1/2}) - F_k(\rho_j^{k,n+1/2}, \mathbf{R}_j^{n+1/2})| \\ &= |F_k(\rho_{j+1}^{k,n+1/2}, \mathbf{R}_{j+1}^{n+1/2}) - F_k(\rho_j^{k,n+1/2}, \mathbf{R}_j^{n+1/2}) - F_k(0, \mathbf{R}_{j+1}^{n+1/2}) + F_k(0, \mathbf{R}_j^{n+1/2})| \\ &\leq \lambda_{\max} \left(\rho_{j+1}^{k,n} + \rho_j^{k,n} + \frac{\Delta t}{2} (|\sigma^k(\rho_j^k, \mathbf{R}_j^k)| + |\sigma^k(\rho_{j+1}^k, \mathbf{R}_{j+1}^k)|) \right). \end{aligned}$$

Similarly, we can estimate

$$\Delta x |\sigma^k(\rho_j^n, \mathbf{R}_j^n)| \leq |F_k(\rho_{j+1}^{k,n}, \mathbf{R}_{j+1}^n) - F_k(\rho_j^{k,n}, \mathbf{R}_j^n)| \leq \lambda_{\max} (\rho_{j+1}^{k,n} + \rho_j^{k,n}).$$

Note that we have the same estimate for $\Delta x |\sigma^k(\rho_{j+1}^n, \mathbf{R}_{j+1}^n)| \leq \lambda_{\max} (\rho_{j+1}^{k,n} + \rho_j^{k,n})$. Hence, we obtain

$$|F_k(\rho_{j+1}^{k,n+1/2}, \mathbf{R}_{j+1}^{n+1/2}) - F_k(\rho_j^{k,n+1/2}, \mathbf{R}_j^{n+1/2})| \leq \lambda_{\max} \left(1 + \lambda_{\max} \frac{\Delta t}{\Delta x} \right) (\rho_{j+1}^{k,n} + \rho_j^{k,n}).$$

This allows us to prove the desired lower bound

$$\begin{aligned} \rho_{j+1/2}^{k,n+1} &\geq \frac{1}{2}(\rho_{j+1}^{k,n} + \rho_j^{k,n}) - \frac{1}{4}|\rho_{j+1}^{k,n} - \rho_j^{k,n}| - \frac{\Delta t}{\Delta x} \lambda_{\max} \left(1 + \lambda_{\max} \frac{\Delta t}{\Delta x} \right) (\rho_{j+1}^{k,n} + \rho_j^{k,n}) \\ &\geq \frac{1}{2}(\rho_{j+1}^{k,n} + \rho_j^{k,n}) - \frac{1}{4}|\rho_{j+1}^{k,n} - \rho_j^{k,n}| - \kappa (1 + \kappa) (\rho_{j+1}^{k,n} + \rho_j^{k,n}) \\ &\geq \frac{1}{2}(\rho_{j+1}^{k,n} + \rho_j^{k,n}) - \frac{1}{4}|\rho_{j+1}^{k,n} - \rho_j^{k,n}| - \frac{1}{4}(\rho_{j+1}^{k,n} + \rho_j^{k,n}) \\ &= \frac{1}{2} \min\{\rho_{j+1}^{k,n}, \rho_j^{k,n}\} \geq 0. \end{aligned}$$

□

Remark 2.7. We note that the proof is similar to the proof of [37, Theorem 4.1] where a local but discontinuous flux is considered. Similar to [37] and under further assumptions on the flux we can obtain stricter lower and upper bounds on the solution. In particular, if there exist a ρ_m such that $\rho_0^k(x) \geq \rho_m$ for $x \in \mathbb{R}$ and $F_k(\rho_m, R) = 0$ for $R \in \mathbb{R}^m$, we obtain the lower bound ρ_m . Similarly, assuming the existence of ρ_M such that $\rho_0^k(x) \leq \rho_M$ for $x \in \mathbb{R}$ and $F_k(\rho_M, R) = 0$ for $R \in \mathbb{R}^m$, gives the upper bound ρ_M . Placing similar assumptions on the source term, e.g. $S_k(\boldsymbol{\rho}, R) = S_k(\rho^k, R)$ with $S_k(\rho_m, R) = S_k(\rho_M, R) = 0$, results can also be obtained for a non-zero source. Further, all the previous statements are still valid for a kernel of compact support without the additional regularity assumptions.

From the positivity we obtain immediately that the NT scheme preserves the L^1 norm.

Corollary 2.8. *For initial data $\boldsymbol{\rho}_0 \in L^1 \cap L^\infty(\mathbb{R}; \mathbb{R}_+^N)$ and under the CFL condition (2.15), the NT schemes (2.14) preserves the L^1 norm in the following sense*

$$\Delta x \sum_{j \in \mathbb{Z}} |\rho_j^{k,n}| = \Delta x \sum_{j \in \mathbb{Z}} |\rho_j^{k,0}|, \quad \text{for } n \in \mathbb{N} \text{ and every } k \in \{1, \dots, N\}.$$

Without further assumptions, there is only an exponential upper bound on the solution. To prove this we first need some estimates on the non-local terms.

Lemma 2.9. *Let $\omega \in C^2 \cap W^{2,\infty}(\mathbb{R}; \mathbb{R}_+^{m \times N})$, then we obtain for $\ell = 1, \dots, m$ and $k = 1, \dots, N$ and $\omega^{\ell,k}$ of compact support the following estimates*

$$|R_{j+1}^{\ell,k,n} - R_j^{\ell,k,n}| \leq C_1 \Delta x \quad \text{and} \quad |R_{t,j+1}^{\ell,k,n} - R_{t,j}^{\ell,k,n}| \leq C_2$$

with $C_1, C_2 > 0$ depending only on $\omega, F, \boldsymbol{\rho}_0$.

Proof. For simplicity, we neglect the indexes ℓ and k during parts of this proof.

$$\begin{aligned} R_{j+1}^n - R_j^n &= \frac{\Delta x}{2} \omega \left(\left(\frac{1}{4} - N_1 \right) \Delta x \right) \left(\rho_{j-N_1+1}^n + \frac{\Delta x}{4} s_{j-N_1+1}^n - \rho_{j-N_1}^n - \frac{\Delta x}{4} s_{j-N_1}^n \right) \\ &\quad + \Delta x \sum_{l=-N_1}^{N_2-2} \omega((l+1)\Delta x) (\rho_{j+l+2}^n - \rho_{j+l+1}^n) \\ &\quad + \frac{\Delta x}{2} \omega \left(\left(N_2 - \frac{1}{4} \right) \Delta x \right) \left(\rho_{j+N_2+1}^n - \frac{\Delta x}{4} s_{j+N_2+1}^n - \rho_{j+N_2}^n + \frac{\Delta x}{4} s_{j+N_2}^n \right) \end{aligned}$$

Due to the regularity assumptions on the kernel and its compact support, $\omega(-N_1\Delta x) = \omega(N_2\Delta x) = 0$ holds. Using this and summation by parts we get

$$\begin{aligned} R_{j+1}^n - R_j^n &= \frac{\Delta x}{2} \left(\omega \left(\left(\frac{1}{4} - N_1 \right) \Delta x \right) - \omega(N_1\Delta x) \right) \left(\rho_{j-N_1+1}^n + \frac{\Delta x}{4} s_{j-N_1+1}^n - \rho_{j-N_1}^n - \frac{\Delta x}{4} s_{j-N_1}^n \right) \\ &\quad + \Delta x \sum_{l=-N_1}^{N_2-2} \rho_{j+l+1}^n (\omega((l+2)\Delta x) - \omega((l+1)\Delta x)) - \Delta x \omega((1-N_1)\Delta x) \rho_{j-N_1+1} \\ &\quad + \frac{\Delta x}{2} \left(\omega \left(\left(N_2 - \frac{1}{4} \right) \Delta x \right) - \omega(N_2\Delta x) \right) \left(\rho_{j+N_2+1}^n - \frac{\Delta x}{4} s_{j+N_2+1}^n - \rho_{j+N_2}^n + \frac{\Delta x}{4} s_{j+N_2}^n \right) \end{aligned}$$

With the mean value theorem on the differences of ω , we get the estimate

$$|R_{j+1}^{\ell,k,n} - R_j^{\ell,k,n}| \leq \Delta x \|\partial_x \omega^{\ell,k}\|_{L^\infty(\mathbb{R}; \mathbb{R})} \frac{5}{2} \|\rho_0^k\|_{L^1(\mathbb{R}; \mathbb{R}_+)}.$$

Analogously, to above we can obtain

$$|R_{t,j+1}^{\ell,k,n} - R_{t,j}^{\ell,k,n}| \leq \|\partial_x \omega^{\ell,k}\|_{L^\infty(\mathbb{R};\mathbb{R})} \frac{5}{2} \Delta x \sum_{j \in \mathbb{Z}} \Delta x |\sigma^k(\boldsymbol{\rho}_j^n, \mathbf{R}_j^n)| \leq \|\partial_x \omega^{\ell,k}\|_{L^\infty(\mathbb{R};\mathbb{R})} 5 \lambda_{\max} \|\rho_0^k\|_{L^1(\mathbb{R};\mathbb{R}^+)}. \quad \square$$

With the help of Lemma 2.9 we are now able to prove an upper bound on the solutions of the NT scheme.

Theorem 2.10. *For initial data $\boldsymbol{\rho}_0 \in L^1 \cap L^\infty(\mathbb{R}; \mathbb{R}_+^N)$ and under the CFL condition (2.15) there exists a $\mathcal{C} \geq 0$ depending only on ω , F , $\boldsymbol{\rho}_0$, M , m and N such that the approximate solutions of the NT scheme satisfy*

$$\rho_j^{k,n} \leq \max_{k=1,\dots,N} \|\rho_0^k\|_{L^\infty(\mathbb{R};\mathbb{R}_+)} \exp(\mathcal{C}t^n)$$

for any $n \in \mathbb{N}$, $j \in \mathbb{Z}$ and $k \in \{1, \dots, N\}$.

Proof. Similar as in the proof of the positivity, it is sufficient to prove the estimate for the staggered approximation. Again, we start with an estimate on the difference of the fluxes. Here, we get

$$\begin{aligned} & |F_k(\rho_{j+1}^{k,n+1/2}, \mathbf{R}_{j+1}^{n+1/2}) - F_k(\rho_j^{k,n+1/2}, \mathbf{R}_j^{n+1/2})| \\ & \leq \lambda_{\max} \left(|\rho_{j+1}^{k,n} - \rho_j^{k,n}| + \frac{\Delta t}{2} (|\sigma^k(\boldsymbol{\rho}_j^n, \mathbf{R}_j^n)| + |\sigma^k(\boldsymbol{\rho}_{j+1}^n, \mathbf{R}_{j+1}^n)|) \right) + \|\nabla_R F_k\| \|\mathbf{R}_{j+1}^{n+1/2} - \mathbf{R}_j^{n+1/2}\|. \end{aligned}$$

Thanks to Lemma 2.9 it becomes apparent that there exists a \tilde{C} depending only on ω , F , $\boldsymbol{\rho}_0$, m and N , such that

$$\|\mathbf{R}_{j+1}^{n+1/2} - \mathbf{R}_j^{n+1/2}\| \leq \tilde{C} \Delta x.$$

Similarly, the estimates of Lemma 2.9 allow us to get a more precise estimate on the slopes of the fluxes, too:

$$\begin{aligned} \Delta x |\sigma^k(\boldsymbol{\rho}_j^n, \mathbf{R}_j^n)| & \leq |F_k(\rho_{j+1}^{k,n}, \mathbf{R}_{j+1}^n) - F_k(\rho_j^{k,n}, \mathbf{R}_j^n)| \\ & \leq \lambda_{\max} |\rho_{j+1}^{k,n} - \rho_j^{k,n}| + \|\nabla_R F_k\| \|\mathbf{R}_{j+1}^n - \mathbf{R}_j^n\| \\ & \leq \lambda_{\max} |\rho_{j+1}^{k,n} - \rho_j^{k,n}| + \tilde{C} \Delta x M \max_{j \in \mathbb{Z}} \rho_j^n. \end{aligned}$$

Here, we also used the assumption on $\nabla_R F_k$. Using it once more and combining the estimates above, we get

$$|F_k(\rho_{j+1}^{k,n+1/2}, \mathbf{R}_{j+1}^{n+1/2}) - F_k(\rho_j^{k,n+1/2}, \mathbf{R}_j^{n+1/2})| \leq \lambda_{\max} \left(\frac{\Delta t}{\Delta x} \lambda_{\max} + 1 \right) |\rho_{j+1}^{k,n} - \rho_j^{k,n}| + \mathcal{C} \Delta x \max_{j \in \mathbb{Z}} \rho_j^n.$$

Therefore, we obtain

$$\begin{aligned} \rho_{j+1/2}^{k,n+1} & \leq \frac{1}{2} (\rho_j^{k,n} + \rho_{j+1}^{k,n}) + \frac{1}{4} |\rho_j^{k,n} - \rho_{j+1}^{k,n}| + \frac{\Delta t}{\Delta x} \lambda_{\max} \left(\frac{\Delta t}{\Delta x} \lambda_{\max} + 1 \right) |\rho_{j+1}^{k,n} - \rho_j^{k,n}| + \mathcal{C} \Delta t \max_{j \in \mathbb{Z}} \rho_j^n \\ & \leq \frac{1}{2} (\rho_j^{k,n} + \rho_{j+1}^{k,n} + |\rho_j^{k,n} - \rho_{j+1}^{k,n}|) + \mathcal{C} \Delta t \max_{j \in \mathbb{Z}} \rho_j^n \\ & \leq (1 + \mathcal{C} \Delta t) \max_{j \in \mathbb{Z}} \rho_j^n. \end{aligned}$$

Applying the formula recursively, we obtain the desired estimate. \square

3 Kurganov-Tadmor fully discrete central scheme

To reduce the numerical diffusion of the NT scheme, the concept of the KT scheme from [36] is to split the original cell into two intervals and to consider a non-smooth and smooth region. Therefore, the local wave speeds at each cell interface are needed, which are in the non-local case not always easy to compute exactly or to estimate. Nevertheless, for the system (2.1) such estimates can be obtained.

We start from the same grid as in the previous section, approximate the initial conditions and cell averages as before, and use the same linear reconstruction in each cell, i.e., equation (2.2). Then we compute the left and right approximations of the cell averages

$$\rho_{j+1/2}^{k,+} = \rho_{j+1}^{k,n} + s_{j+1}^{k,n}(x_{j+1/2} - x_{j+1}), \quad \rho_{j+1/2}^{k,-} = \rho_j^{k,n} + s_j^{k,n}(x_{j+1/2} - x_j).$$

We note that at each cell interface the non-local term $\mathbf{R}(t, x)$ is continuous such that for the system (2.1) we can estimate the local speeds by

$$c_{j+1/2}^n = \max_{k=1, \dots, N} \max \left\{ \frac{\partial F_k}{\partial \rho} \left(\rho_{j+1/2}^{k,-}, \mathbf{R}_{j+1/2}^n \right), \frac{\partial F_k}{\partial \rho} \left(\rho_{j+1/2}^{k,+}, \mathbf{R}_{j+1/2}^n \right) \right\}, \quad (3.1)$$

with $\mathbf{R}_{j+1/2}^n$ as an approximation of $\mathbf{R}(t^n, x_{j+1/2})$, i.e., for $\ell = 1, \dots, m$, $k = 1, \dots, N$

$$R^{\ell,k}(t^n, x_{j+1/2}) = \Delta x \sum_{l=-N_1^k}^{N_2^k} \rho_{j+l}^{k,n} \omega^{\ell,k}((l+1/2)\Delta x).$$

The main idea that the non-local term is continuous at the cell-interface and only needs to be approximated there was already used for first-order schemes in [24, 25].

Using the local speed $c_{j+1/2}^n$ we can separate each interval into a non-smooth part around the cell interface and a smooth part. As in [36], the non-smooth region is given by $[x_{j+1/2,l}^n, x_{j+1/2,r}^n]$ and the smooth region by $[x_{j-1/2,r}^n, x_{j+1/2,l}^n]$, where

$$x_{j+1/2,l}^n = x_{j+1/2} - c_{j+1/2}^n \Delta t, \quad \text{and} \quad x_{j+1/2,r}^n = x_{j+1/2} + c_{j+1/2}^n \Delta t.$$

In particular, we now use narrower control volumes than in the NT scheme: the points $x_{j+1/2,l}^n = x_{j+1/2} - c_{j+1/2}^n \Delta t$ and $x_{j+1/2,r}^n = x_{j+1/2} + c_{j+1/2}^n \Delta t$ separate between smooth and non-smooth regions, see Figure 2, and hence the non-smooth parts of the solution are contained inside narrower control volumes of spatial width $2c_{j+1/2}^n \Delta t$. In the next step, we proceed similar to the NT scheme by integrating in each time step over the interval, but treat the smooth and non-smooth parts separately.

3.1 Non-smooth region

We start with the integration of the balance law (2.1) over the non-smooth region, i.e., over the non-uniform rectangles, $[x_{j+1/2,l}^n, x_{j+1/2,r}^n] \times [t^n, t^{n+1}]$. Let us define $\Delta x_{j+1/2} = x_{j+1/2,r}^n -$

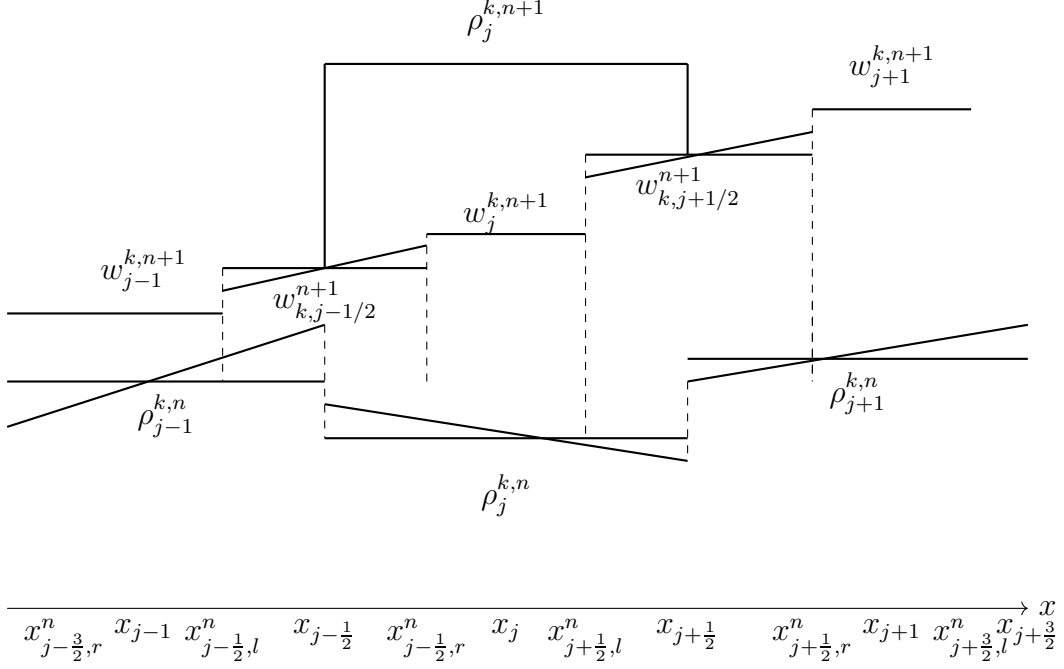


Figure 2: Fully discrete KT scheme reconstruction for fixed $k \in \{1, \dots, N\}$, compare Figure 3.2 from [36]

$x_{j+1/2,l}^n = 2c_{j+1/2}^n \Delta t$. This gives the intermediate cell-averages at t^{n+1} .

$$\begin{aligned}
w_{j+1/2}^{k,n+1} &= \frac{1}{\Delta x_{j+1/2}} \int_{x_{j+1/2,l}^n}^{x_{j+1/2,r}^n} \rho^k(t^{n+1}, x) dx, \\
&= \frac{1}{\Delta x_{j+1/2}} \left[\int_{x_{j+1/2,l}^n}^{x_{j+1/2}} \tilde{\rho}_j^k(t^n, x) dx + \int_{x_{j+1/2}}^{x_{j+1/2,r}^n} \tilde{\rho}_{j+1}^k(t^n, x) dx \right] \\
&\quad - \frac{1}{\Delta x_{j+1/2}} \int_{t^n}^{t^{n+1}} \left(F_k(\rho^k(t, x_{j+1/2,r}^n), \mathbf{R}(t, x_{j+1/2,r}^n)) - F_k(\rho^k(t, x_{j+1/2,l}^n), \mathbf{R}(t, x_{j+1/2,l}^n)) \right) dt \\
&\quad + \frac{1}{\Delta x_{j+1/2}} \int_{t^n}^{t^{n+1}} \int_{x_{j+1/2,l}^n}^{x_{j+1/2,r}^n} S_k(\tilde{\rho}(t, x), \mathbf{R}(t, x)) dx dt, \\
&= \frac{\rho_j^{k,n} + \rho_{j+1}^{k,n}}{2} + \frac{\Delta x - c_{j+1/2}^n \Delta t}{4} (s_j^{k,n} - s_{j+1}^{k,n}) - \frac{1}{2c_{j+1/2}^n} [F_k(\rho_{j+1/2,r}^{k,n+1/2}, \mathbf{R}_{j+1/2,r}^{n+1/2}) - F_k(\rho_{j+1/2,l}^{k,n+1/2}, \mathbf{R}_{j+1/2,l}^{n+1/2})] \\
&\quad + \frac{\Delta t}{2} \left[S_k(\rho_{j+1/2,r}^{n+1/2}, \mathbf{R}_{j+1/2,r}^{n+1/2}) + S_k(\rho_{j+1/2,l}^{n+1/2}, \mathbf{R}_{j+1/2,l}^{n+1/2}) \right].
\end{aligned}$$

As in the NT scheme we used the midpoint rule for the flux integrals, and midpoint rule in time and trapezoidal rule in space for the source term. Here, the midpoint values are obtained

again from the corresponding Taylor expansions:

$$\begin{aligned}
\rho_{j+1/2,l}^{k,n+1/2} &= \rho_{j+1/2,l}^{k,n} - \frac{\Delta t}{2} \sigma^k(\rho_{j+1/2,l}^n, \mathbf{R}_{j+1/2,l}^n) + \frac{\Delta t}{2} S_k(\rho_{j+1/2,l}^n, \mathbf{R}_{j+1/2,l}^n), \\
\rho_{j+1/2,l}^{k,n} &= \rho_j^{k,n} + s_j^{k,n} \left(\frac{\Delta x}{2} - \Delta t c_{j+1/2}^n \right), \\
\rho_{j+1/2,r}^{k,n+1/2} &= \rho_{j+1/2,r}^{k,n} - \frac{\Delta t}{2} \sigma^k(\rho_{j+1/2,r}^n, \mathbf{R}_{j+1/2,r}^n) + \frac{\Delta t}{2} S_k(\rho_{j+1/2,r}^n, \mathbf{R}_{j+1/2,r}^n), \\
\rho_{j+1/2,r}^{k,n} &= \rho_{j+1}^{k,n} - s_{j+1}^{k,n} \left(\frac{\Delta x}{2} - \Delta t c_{j+1/2}^n \right).
\end{aligned} \tag{3.2}$$

The derivatives are approximated by

$$\begin{aligned}
&\sigma^k(\rho_{j+1/2,l}^n, \mathbf{R}_{j+1/2,l}^n) \\
&= \text{minmod} \left(\frac{F_k(\rho_{j+1/2,l}^{k,n}, \mathbf{R}_{j+1/2,l}^n) - F_k(\rho_{j-1/2,l}^{k,n}, \mathbf{R}_{j-1/2,l}^n)}{\Delta x - c_{j-1/2}^n \Delta t + c_{j+1/2}^n \Delta t}, \frac{F_k(\rho_{j+3/2,l}^{k,n}, \mathbf{R}_{j+3/2,l}^n) - F_k(\rho_{j+1/2,l}^{k,n}, \mathbf{R}_{j+1/2,l}^n)}{\Delta x - c_{j+1/2}^n \Delta t + c_{j+3/2}^n \Delta t} \right), \\
&\sigma^k(\rho_{j+1/2,r}^n, \mathbf{R}_{j+1/2,r}^n) \\
&= \text{minmod} \left(\frac{F_k(\rho_{j+1/2,r}^{k,n}, \mathbf{R}_{j+1/2,r}^n) - F_k(\rho_{j-1/2,r}^{k,n}, \mathbf{R}_{j-1/2,r}^n)}{\Delta x + c_{j-1/2}^n \Delta t - c_{j+1/2}^n \Delta t}, \frac{F_k(\rho_{j+3/2,r}^{k,n}, \mathbf{R}_{j+3/2,r}^n) - F_k(\rho_{j+1/2,r}^{k,n}, \mathbf{R}_{j+1/2,r}^n)}{\Delta x + c_{j+1/2}^n \Delta t - c_{j+3/2}^n \Delta t} \right),
\end{aligned}$$

and the flux can be computed by using the non-local terms, detailed below in (3.3) and (3.4). We calculate $\mathbf{R}_{j+1/2,r/l}^{n+1/2}$ similar as in the NT scheme by using the Taylor series expansion,

$$\mathbf{R}(t^{n+1/2}, x_{j+1/2,r/l}^n) \approx \mathbf{R}(t^n, x_{j+1/2,r/l}^n) + \frac{\Delta t}{2} \mathbf{R}_t(t^n, x_{j+1/2,r/l}^n).$$

Thereby, the terms $\mathbf{R}_{j+1/2,r/l}$, $\mathbf{R}_t(t^n, x_{j+1/2,r/l}^n)$ are approximated using a midpoint quadrature rule. For simplicity, we will again neglect the index ℓ and set $m = 1$:

$$\begin{aligned}
&R^k(t^n, x_{j+1/2,l}^n) \tag{3.3} \\
&\approx \int_{x_{j+1/2-N_1^k}^n}^{x_{j+1/2-N_1^k}^n} \omega_\eta^k(y - x_{j+1/2,l}^n) \tilde{\rho}_{j-N_1^k}^k(t^n, y) dy + \sum_{l=-N_1^k}^{N_2^k-2} \int_{x_{j+1/2+l}^n}^{x_{j+3/2+l}^n} \omega_\eta^k(y - x_{j+1/2,l}^n) \tilde{\rho}_{j+l+1}^k(t^n, y) dy \\
&+ \int_{x_{j+N_2^k-1/2}^n}^{x_{j+1/2+N_2^k,l}^n} \omega_\eta^k(y - x_{j+1/2,l}^n) \tilde{\rho}_{j+N_2^k}^k(t^n, y) dy, \\
&= c_{j+1/2}^n \Delta t \omega_\eta^k \left(\frac{c_{j+1/2}^n \Delta t}{2} - N_1^k \Delta x \right) \left(\rho_{j-N_1^k}^{k,n} + \frac{\Delta x - c_{j+1/2}^n \Delta t}{2} s_{j-N_1^k}^{k,n} \right) \\
&+ \sum_{l=-N_1^k}^{N_2^k-2} \Delta x \omega_\eta^k((l+1/2)\Delta x + c_{j+1/2}^n \Delta t) \rho_{j+l+1}^{k,n} \\
&+ (\Delta x - c_{j+1/2}^n \Delta t) \omega_\eta^k \left(\frac{(2N_2^k-1)\Delta x + c_{j+1/2}^n \Delta t}{2} \right) \left(\rho_{j+N_2^k}^{k,n} - \frac{c_{j+1/2}^n \Delta t}{2} s_{j+N_2^k}^{k,n} \right).
\end{aligned}$$

Similarly, we obtain

$$\begin{aligned}
R^k(t^n, x_{j+1/2,r}^n) &\approx (\Delta x - c_{j+1/2}^n \Delta t) \omega_\eta^k \left(\frac{\Delta x - c_{j+1/2}^n \Delta t}{2} - N_1^k \Delta x \right) \left(\rho_{j+1-N_1^k}^{k,n} + \frac{c_{j+1/2}^n \Delta t}{2} s_{j+1-N_1^k}^{k,n} \right) \\
&\quad + \sum_{l=-N_1^k}^{N_2^k-2} \Delta x \omega_\eta^k ((l+3/2)\Delta x - c_{j+1/2}^n \Delta t) \rho_{j+l+2}^{k,n} \\
&\quad + c_{j+1/2}^n \Delta t \omega_\eta \left(\frac{2N_2^k \Delta x - c_{j+1/2}^n \Delta t}{2} \right) \left(\rho_{j+N_2^k+1}^{k,n} - \frac{\Delta x - c_{j+1/2}^n \Delta t}{2} s_{j+N_2^k+1}^{k,n} \right). \tag{3.4}
\end{aligned}$$

To approximate $R_t^k(t^n, x_{j+1/2,r/l}^n)$ we use a first order quadrature rule. For the first and last cell we follow the idea of Remark 2.3 and for the cells in between we evaluate the reconstruction at $x_{j+1/2,r/l}^n$ and the kernel at the midpoint. This keeps the computational cost low by using already computed values and is a first order accurate approximation:

$$\begin{aligned}
R_t^k(t^n, x_{j+1/2,r}^n) &\approx \int_{x_{j+1/2-N_1^k,r}^n}^{x_{j+1/2+N_2^k,r}^n} \omega_\eta^k(y - x_{j+1/2,r}^n) \left(S_k(\tilde{\rho}(t^n, y), \mathbf{R}(t^n, y)) - \sigma^k(\rho(t^n, y), \mathbf{R}(t^n, y)) \right) dy, \\
&= (\Delta x - \Delta t c_{j+1/2}^n) \omega_\eta^k \left(\frac{\Delta x - c_{j+1/2}^n \Delta t}{2} - N_1^k \Delta x \right) \left(S_k(\rho_{j+1/2-N_1^k,r}^n, \mathbf{R}_{j+1/2-N_1^k,r}^n) \right. \\
&\quad \left. - \sigma^k(\rho_{j+1/2-N_1^k,r}^n, \mathbf{R}_{j+1/2-N_1^k,r}^n) \right) \\
&\quad + \sum_{l=-N_1^k}^{N_2^k-2} \Delta x \omega_\eta^k ((l+3/2)\Delta x - c_{j+1/2}^n \Delta t) \left(S_k(\rho_{j+3/2+l,r}^n, \mathbf{R}_{j+3/2+l,r}^n) - \sigma^k(\rho_{j+3/2+l,r}^n, \mathbf{R}_{j+3/2+l,r}^n) \right) \\
&\quad + c_{j+1/2}^n \Delta t \omega_\eta \left(\frac{2N_2^k \Delta x - c_{j+1/2}^n \Delta t}{2} \right) \left(S_k(\rho_{j+1/2+N_2^k,r}^n, \mathbf{R}_{j+1/2+N_2^k,r}^n) - \sigma^k(\rho_{j+1/2+N_2^k,r}^n, \mathbf{R}_{j+1/2+N_2^k,r}^n) \right),
\end{aligned}$$

and

$$\begin{aligned}
R_t^k(t^n, x_{j+1/2,l}^n) &\approx c_{j+1/2}^n \Delta t \omega_\eta^k \left(\frac{c_{j+1/2}^n \Delta t}{2} - N_1^k \Delta x \right) \left(S_k(\rho_{j+1/2-N_1^k,l}^n, \mathbf{R}_{j+1/2-N_1^k,l}^n) - \sigma^k(\rho_{j+1/2-N_1^k,l}^n, \mathbf{R}_{j+1/2-N_1^k,l}^n) \right) \\
&\quad + \sum_{l=-N_1^k}^{N_2^k-2} \Delta x \omega_\eta^k ((l+1/2)\Delta x + c_{j+1/2}^n \Delta t) \left(S_k(\rho_{j+3/2+l,l}^n, \mathbf{R}_{j+3/2+l,l}^n) - \sigma^k(\rho_{j+3/2+l,l}^n, \mathbf{R}_{j+3/2+l,l}^n) \right) \\
&\quad + (\Delta x - c_{j+1/2}^n \Delta t) \omega_\eta^k \left(\frac{(2N_2^k - 1)\Delta x + c_{j+1/2}^n \Delta t}{2} \right) \left(S_k(\rho_{j+1/2+N_2^k,l}^n, \mathbf{R}_{j+1/2+N_2^k,l}^n) \right. \\
&\quad \left. - \sigma^k(\rho_{j+1/2+N_2^k,l}^n, \mathbf{R}_{j+1/2+N_2^k,l}^n) \right).
\end{aligned}$$

3.2 Smooth region

For the smooth region, we integrate over $[x_{j-1/2,r}^n, x_{j+1/2,l}^n] \times [t^n, t^{n+1}]$ and define $\Delta x_j = x_{j+1/2,l}^n - x_{j-1/2,r}^n = \Delta x - \Delta t(c_{j-1/2}^n + c_{j+1/2}^n)$, which gives the following intermediate cell-averages at t^{n+1}

$$\begin{aligned}
w_j^{k,n+1} &= \frac{1}{\Delta x_j} \int_{x_{j-1/2,r}^n}^{x_{j+1/2,l}^n} \rho^k(t^{n+1}, x) dx, \\
&= \frac{1}{\Delta x_j} \int_{x_{j-1/2,r}^n}^{x_{j+1/2,l}^n} \tilde{\rho}_j^k(t^n, x) dx + \frac{1}{\Delta x_j} \int_{t^n}^{t^{n+1}} \int_{x_{j-1/2,r}^n}^{x_{j+1/2,l}^n} S_k(\tilde{\rho}(t, x), \mathbf{R}(t, x)) dx dt \\
&\quad - \frac{1}{\Delta x_j} \int_{t^n}^{t^{n+1}} \left(F_k(\rho^k(t, x_{j+1/2,l}^n), \mathbf{R}(t, x_{j+1/2,l}^n)) - F_k(\rho^k(t, x_{j-1/2,r}^n), \mathbf{R}(t, x_{j-1/2,r}^n)) \right) dt, \\
&= \rho_j^{k,n} + \frac{\Delta t}{4} (c_{j+1/2}^n - c_{j-1/2}^n) s_j^{k,n} + \frac{\Delta t}{2} \left[S_k(\rho_{j+1/2,l}^{n+1/2}, \mathbf{R}_{j+1/2,l}^{n+1/2}) + S_k(\rho_{j-1/2,r}^{n+1/2}, \mathbf{R}_{j-1/2,r}^{n+1/2}) \right] \\
&\quad - \frac{\Delta t}{\Delta x - \Delta t(c_{j+1/2}^n + c_{j-1/2}^n)} \left[F_k(\rho_{j+1/2,l}^{k,n+1/2}, \mathbf{R}_{j+1/2,l}^{n+1/2}) - F_k(\rho_{j-1/2,r}^{k,n+1/2}, \mathbf{R}_{j-1/2,r}^{n+1/2}) \right].
\end{aligned}$$

The intermediate values can be obtained by (3.2) and the formulas above.

3.3 Projection

The solution at time level $t = t^{n+1}$ is now expressed in terms of the approximate cell averages, $w_{j+1/2}^{k,n+1}$, $w_j^{k,n+1}$, which spread over a non-uniform grid twice the number of the original cells at $t = t^n$. To obtain the cell averages over the original uniform grid with non-staggered cells $[x_{j-1/2}, x_{j+1/2}]$, we consider a piecewise-linear reconstruction over the non-uniform cells at $t = t^{n+1}$, and following [31], we project its averages back onto the original uniform grid. Note that it is not necessary to calculate a piecewise-linear reconstruction of the smooth part, i.e., $w_j^{k,n+1}$, as it will be averaged out, see Figure 2. Hence as in [36], the required piecewise-linear approximation takes the form

$$\tilde{w}^k(t^{n+1}, x) = \sum_j \left[w_{j+1/2}^{k,n+1} + s_{j+1/2}^{k,n+1} (x - x_{j+1/2}) \right] \chi_{[x_{j+1/2,r}^n, x_{j+1/2,l}^n]}(x) + w_j^{k,n+1} \chi_{[x_{j-1/2,r}^n, x_{j+1/2,l}^n]}(x), \quad (3.5)$$

where

$$s_{j+1/2}^{k,n+1} = \frac{2}{\Delta x} \text{minmod} \left(\frac{w_{j+1}^{k,n+1} - w_{j+1/2}^{n+1}}{1 + \frac{\Delta t}{\Delta x} (c_{j+1/2}^n - c_{j+3/2}^n)}, \frac{w_{j+1/2}^{k,n+1} - w_j^{k,n+1}}{1 + \frac{\Delta t}{\Delta x} (c_{j+1/2}^n - c_{j-1/2}^n)} \right).$$

Finally, the desired cell averages, $\rho_j^{k,n+1}$, are obtained by averaging the approximate solution in (3.5). This results in the following fully discrete second-order central scheme after integrating over the interval $[x_{j-1/2}, x_{j+1/2}]$

$$\begin{aligned}
\rho_j^{k,n+1} &= \frac{1}{\Delta x} \int_{x_{j-1/2}}^{x_{j+1/2}} \tilde{w}^k(t^{n+1}, x) dx, \\
&= \frac{\Delta t}{\Delta x} c_{j-1/2}^n w_{j-1/2}^{k,n+1} + \left[1 - \frac{\Delta t}{\Delta x} (c_{j-1/2}^n + c_{j+1/2}^n) \right] w_j^{k,n+1} + \frac{\Delta t}{\Delta x} c_{j+1/2}^n w_{j+1/2}^{k,n+1} \\
&\quad + \frac{\Delta x}{2} \left[\left(\frac{\Delta t}{\Delta x} c_{j-1/2}^n \right)^2 s_{j-1/2}^{k,n+1} - \left(\frac{\Delta t}{\Delta x} c_{j+1/2}^n \right)^2 s_{j+1/2}^{k,n+1} \right].
\end{aligned} \quad (3.6)$$

4 Numerical examples

In this section, we demonstrate the applicability and performance of the central schemes of Sections 2 and 3 to different models. We also show how to apply them to further non-local models not covered in the previous sections.

We will present convergence tests for smooth initial data and an approximation of the solution for discontinuous initial data to demonstrate the performance of the numerical schemes. If not stated otherwise, we use periodic boundary conditions.

4.1 Scalar case

In the first test case, we demonstrate how the schemes perform in the presence of a nonlinearity in the flux. Since the NT and KT schemes belong to the class of central schemes (as the LxF), they can be directly applied to models with a nonlinearity in the flux and no Riemann solvers need to be constructed. Here, we consider the scalar case, so that we can compare the solution with the approximation of Godunov-type scheme, which involves solving a maximization/minimization problem.

In particular, we consider the non-local Arrhenius-type look ahead dynamics for $N = 1$ similar to [8, 14, 40]:

$$\partial_t \rho + \partial_x (\rho(1 - \rho)v(\omega_\eta * \rho)) = 0,$$

with $v(\rho) = \exp(-\rho)$ and a kernel function of compact support on $[0, \eta]$, non-increasing and unit integral. Godunov and Lax-Friedrichs-type schemes for this and similar models have already been discussed in several works, see e.g. [14, 24, 25, 30]. Here, we employ the schemes considered in [25].

In the following, the non-local range is set to $\eta = 0.2$. The discontinuous initial condition $\rho_0(x)$ is given by

$$\rho_0(x) = 0.2 + 0.8\chi_{[-1/4, 1/4]}(x), \quad (4.1)$$

and the kernel is constant, i.e., $\omega_\eta(x) = 1/\eta$ for $x \in [0, \eta]$. Figure 3 shows the solution at $T = 1.5$ for the different numerical schemes, i.e., the second order accurate NT and KT schemes as well as first order accurate approximations with the grid size $\Delta x = \frac{1}{20} \cdot 2^{-1}$. In addition, a reference solution with the NT scheme and $\Delta x = \frac{1}{20} \cdot 2^{-5}$ is displayed. It can be obtained that the NT scheme provides a more accurate approximation than the LxF scheme, and the KT scheme the most accurate one, followed by the Godunov-type scheme. Note that for smaller step-sizes the NT scheme will be more accurate than the Godunov-type scheme due to its second-order accuracy.

Furthermore, we test the numerical convergence rate in the L^1 -norm. Here, we compare the approximate solutions to a reference solution, still computed by the NT type scheme and $\Delta x = \frac{1}{20} \cdot 2^{-7}$. We consider the smooth initial data

$$\rho_0(x) = 0.5 + 0.4 \sin(\pi x), \quad (4.2)$$

and $\Delta x = \frac{1}{20} \cdot 2^{-n}$ for $n = 0, \dots, 5$. Additionally, we consider the following kernels with compact support on $[0, \eta]$

$$\text{constant: } \omega_\eta(x) = \frac{1}{\eta}, \quad \text{linear: } \omega_\eta(x) = \frac{2}{\eta} \left(1 - \frac{x}{\eta}\right), \quad \text{concave: } \omega_\eta(x) = 3 \frac{\eta^2 - x^2}{2\eta^3}.$$

We note that the convergence to the entropy solution is so far only proven for the LxF and Godunov-type schemes. Nevertheless, Table 1, which shows the corresponding L^1 -errors,

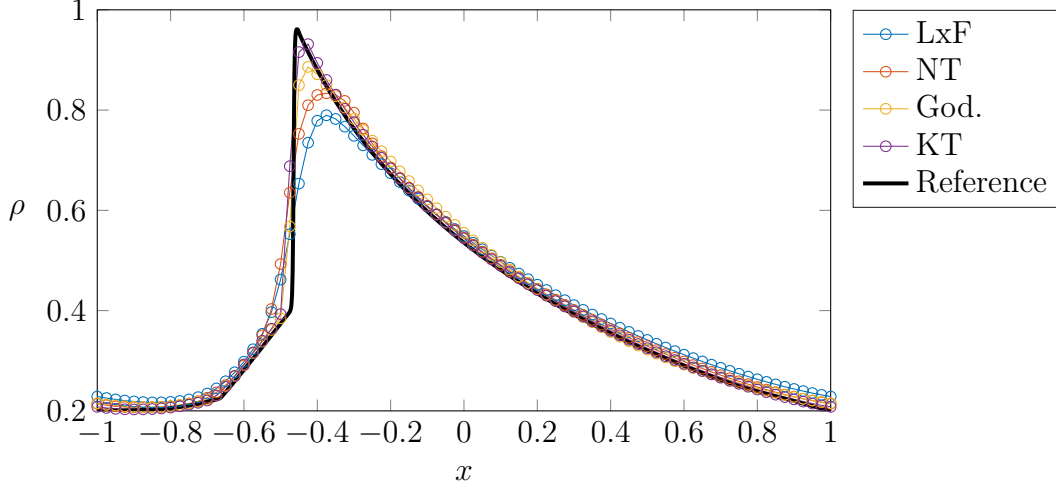


Figure 3: Numerical solutions of the Arrhenius-type look ahead dynamics at $T = 1.5$ obtained by different numerical schemes.

demonstrates that the LxF and Godunov-type scheme converge to the reference solution (with an expected order of one). Hence, the NT (and KT) approximate the correct entropy solution, too. Furthermore, the numerical convergence rates suggest the expected order two for the NT and KT schemes. In particular, the KT scheme always gives the most accurate approximation (as expected by its construction). In contrast to the discontinuous examples the NT scheme is more accurate than the first-order Godunov-type scheme for all step sizes (and kernels).

Table 1: L^1 errors and convergence rates for the smooth initial data and the Arrhenius-type model

	n	LxF		NT		God		KT	
		L^1 error	c.r.	L^1 error	c.r.	L^1 error	c.r.	L^1 error	c.r.
const.	0	1.50e-02	-	6.03e-03	-	7.62e-03	-	1.44e-03	-
	1	6.73e-03	1.16	1.42e-03	2.09	3.99e-03	0.93	3.85e-04	1.90
	2	3.16e-03	1.09	3.65e-04	1.96	1.99e-03	1.00	1.03e-04	1.90
	3	1.53e-03	1.05	9.43e-05	1.95	9.96e-04	1.00	2.78e-05	1.89
	4	7.52e-04	1.02	2.45e-05	1.95	4.97e-04	1.00	7.40e-06	1.91
	5	3.72e-04	1.01	6.15e-06	2.00	2.48e-04	1.00	1.74e-06	2.09
linear	0	1.80e-02	-	6.40e-03	-	7.86e-03	-	1.35e-03	-
	1	7.66e-03	1.23	1.51e-03	2.09	4.10e-03	0.94	3.54e-04	1.93
	2	3.44e-03	1.16	3.67e-04	2.04	2.04e-03	1.01	9.25e-05	1.94
	3	1.62e-03	1.09	9.10e-05	2.01	1.02e-03	1.00	2.41e-05	1.94
	4	7.81e-04	1.05	2.29e-05	1.99	5.08e-04	1.00	6.28e-06	1.94
	5	3.84e-04	1.03	5.67e-06	2.02	2.54e-04	1.00	1.44e-06	2.13
concave	0	1.69e-02	-	6.44e-03	-	7.80e-03	-	1.38e-03	-
	1	7.28e-03	1.22	1.44e-03	2.16	4.06e-03	0.94	3.54e-04	1.96
	2	3.32e-03	1.13	3.62e-04	1.99	2.02e-03	1.01	9.37e-05	1.92
	3	1.58e-03	1.07	9.13e-05	1.99	1.01e-03	1.00	2.47e-05	1.92
	4	7.70e-04	1.04	2.32e-05	1.98	5.05e-04	1.00	6.50e-06	1.93
	5	3.80e-04	1.02	5.77e-06	2.01	2.52e-04	1.00	1.50e-06	2.11

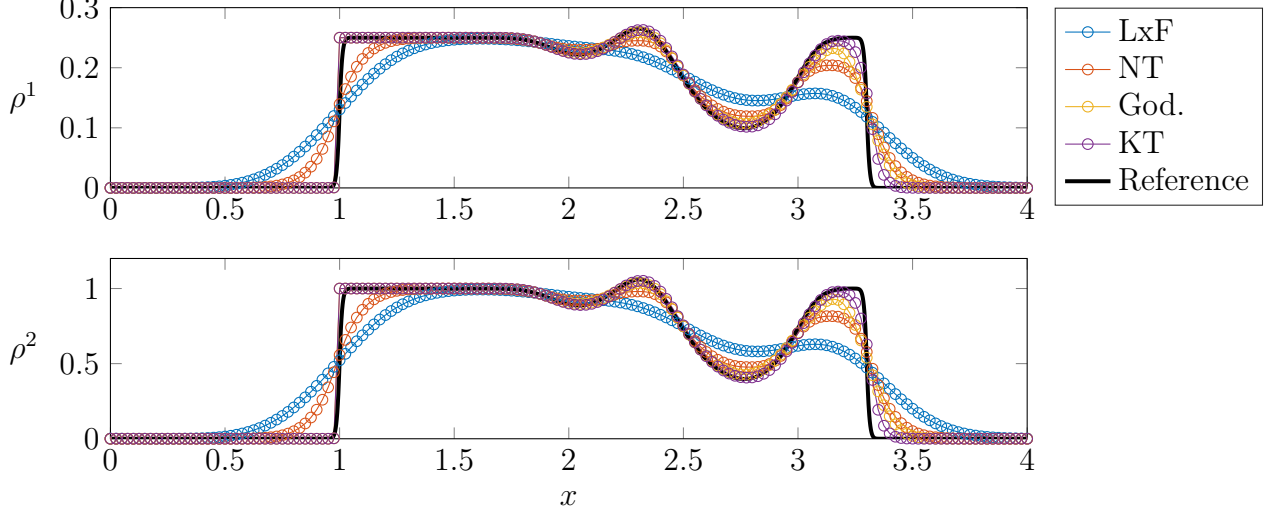


Figure 4: Numerical solutions of the non-local Keyfitz-Kranzer model at $T = 0.3$ obtained by different numerical schemes.

4.2 Keyfitz-Kranzer-Model

As a next test case we consider the Keyfitz-Kranzer model similar to [1, 2]. The modeling equations are given by:

$$\begin{aligned}\partial_t \rho^1 + \partial_x(\rho^1 v(\omega_\eta * \rho^1, \omega_\eta * \rho^2)) &= 0, \\ \partial_t \rho^2 + \partial_x(\rho^2 v(\omega_\eta * \rho^1, \omega_\eta * \rho^2)) &= 0.\end{aligned}$$

The convergence of a Lax-Friedrichs type scheme has been studied in [1] and also the Godunov-type scheme of [24] has been adapted to the system case in [2] and its convergence is proven there. Following [2], we consider the kernel:

$$\omega_\eta(x) = L(-x(\eta + x))^{5/2} \chi_{(-\eta, 0)}(x),$$

where L is chosen such that the integral is normalized to 1. The velocity function is given by: $v(a, b) = (1 - a^2 - b^2)^3$. Again, we consider a discontinuous example to see the approximation of the different numerical schemes. The initial conditions are given by

$$\rho_0^1(x) = 0.25 \chi_{(1,3)}(x), \quad \rho_0^2(x) = \chi_{(1,3)}(x),$$

with $x \in [0, 4]$, the final time is $T = 0.3$ and $\eta = 1$. The solution is given in Figure 4. As in the scalar case all schemes approximate the solution with the LxF scheme being the most diffusive and the KT scheme the most accurate approximation. Note that the grid size is as before $\Delta x = \frac{1}{20} \cdot 2^{-1}$ and the reference solution is computed by the NT scheme and $\Delta x = \frac{1}{20} \cdot 2^{-7}$. The order of accuracy is tested for the smooth initial data

$$\rho_0^1(x) = -0.1 - 0.2 \sin(\pi x), \quad \rho_0^2(x) = 0.2 + 0.1 \sin(\pi x),$$

on the interval $[-1, 1]$ with $\eta = 0.5$ and final time $T = 0.15$. The results in Table 2 display the expected order of accuracy for each numerical scheme.

Table 2: L^1 errors and convergence rates for the smooth initial data and the Keyfitz-Kranzer system

n	LxF		NT		God		KT	
	L^1 -error	c.r.	L^1 -error	c.r.	L^1 -error	c.r.	L^1 -error	c.r.
0	8.53e-02	-	1.77e-02	-	1.13e-02	-	1.65e-03	-
1	4.56e-02	0.90	5.51e-03	1.68	5.68e-03	1.00	4.57e-04	1.85
2	2.37e-02	0.95	1.56e-03	1.82	2.85e-03	1.00	1.20e-04	1.93
3	1.21e-02	0.97	4.24e-04	1.88	1.42e-03	1.00	3.02e-05	1.99
4	6.09e-03	0.99	1.09e-04	1.96	7.12e-04	1.00	6.75e-06	2.16
5	3.06e-03	0.99	2.66e-05	2.03	3.56e-04	1.00	8.83e-07	2.93

4.3 Non-local systems with source term

4.3.1 Multilane traffic flow model

We start by considering a system used to model multilane traffic flow introduced in [5, 22] for simplicity with $N = 2$:

$$\begin{aligned}\partial_t \rho^1 + \partial_x(\rho^1 v(\omega_\eta * \rho^1)) &= -S(\rho^1, \rho^2, \omega_\eta * \rho^1, \omega_\eta * \rho^2), \\ \partial_t \rho^2 + \partial_x(\rho^2 v(\omega_\eta * \rho^2)) &= S(\rho^1, \rho^2, \omega_\eta * \rho^1, \omega_\eta * \rho^2),\end{aligned}$$

and the source term is given similar to [22] as

$$S(\rho^1, \rho^2, R^1, R^2) = (v(R^2) - v(R^1)) \begin{cases} \rho^1(1 - \rho^2), & \text{if } v(R^2) \geq v(R^1), \\ \rho^2(1 - \rho^1), & \text{if } v(R^2) < v(R^1). \end{cases}$$

The kernel is forward looking with compact support on $[0, \eta]$ with unit integral. Here, we consider the linear decreasing kernel with $\eta = 0.5$ and the following test case from [5, 22]:

$$\rho_0^1(x) = q(2x - 0.5), \quad \rho_0^2(x) = q(2x)$$

with

$$q(x) = 4x^2(1 - x^2)\chi_{(0,1)}(x).$$

The solution at $T = 0.5$ is displayed in Figure 5 with $\Delta x = 10^{-2}$. Note that in this example we compute the solution on whole \mathbb{R} and the reference solution is obtained with $\Delta x = 10^{-3}$ and the KT scheme. Similarly as before, the KT scheme gives the most accurate solution.

The smooth initial data to test the convergence are given by

$$\rho_0^1(x) = 0.5 + 0.5 \sin(\pi x), \quad \rho_0^2(x) = 0.25 + 0.25 \cos(2\pi x),$$

on the interval $[-1, 1]$ with the final time $T = 0.15$. Here, the step sizes are given by $\Delta x = \frac{1}{20} \cdot 2^{-n}$, $n = 0, \dots, 5$ and $n = 7$ for the reference solution obtained by the NT scheme. The expected convergence orders can be seen in Table 3.

4.3.2 Non-local Euler equations

Recently in [10], a non-local extension of the Euler equation with relaxation was derived. In one space dimension the equations read:

$$\begin{aligned}\partial_t \rho + \partial_x(\rho(\omega * u)) &= 0, \\ \partial_t u + u \partial_x u &= \rho(\omega * u - u).\end{aligned}\tag{4.3}$$

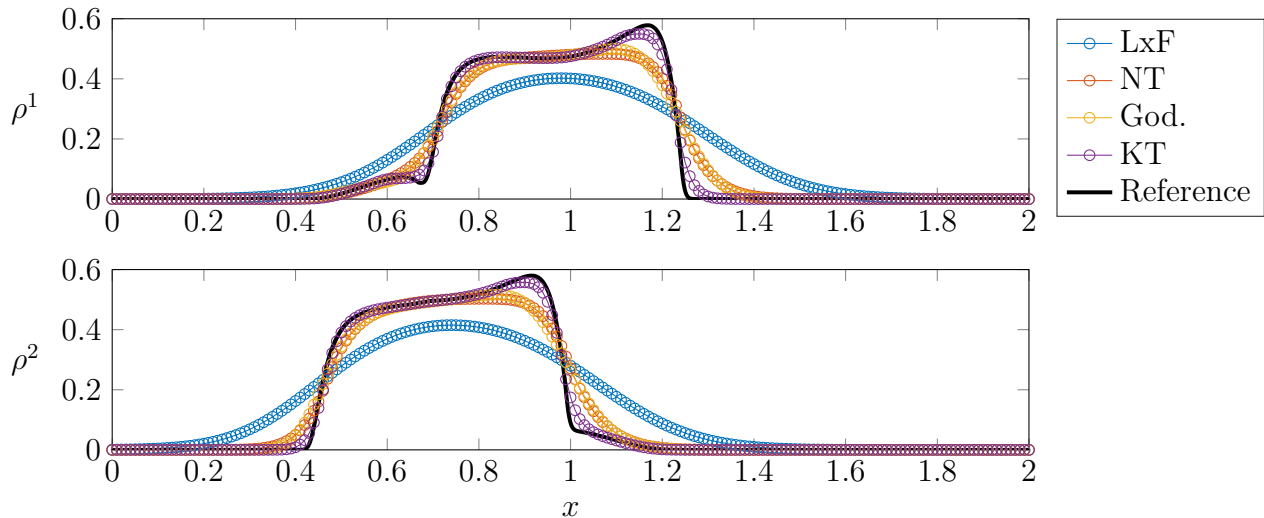


Figure 5: Numerical solutions of the non-local multilane model at $T = 0.5$ obtained by different numerical schemes.

Table 3: L^1 errors and convergence rates for the smooth initial data and the multilane model.

n	LxF		NT		God		KT	
	L^1 -error	c.r.	L^1 -error	c.r.	L^1 -error	c.r.	L^1 -error	c.r.
0	3.14e-01	-	9.78e-02	-	5.05e-02	-	1.22e-02	-
1	1.85e-01	0.76	3.21e-02	1.61	2.59e-02	0.96	3.54e-03	1.79
2	1.02e-01	0.86	1.05e-02	1.62	1.31e-02	0.98	9.98e-04	1.83
3	5.38e-02	0.92	2.96e-03	1.82	6.60e-03	0.99	2.68e-04	1.90
4	2.77e-02	0.96	8.17e-04	1.86	3.31e-03	1.00	6.97e-05	1.94
5	1.41e-02	0.98	2.18e-04	1.90	1.66e-03	1.00	1.74e-05	2.00

Here, a symmetric kernel with unit integral is considered. We consider a symmetric linear kernel defined by

$$\omega(x) = \frac{\eta - |x|}{\eta^2} \chi_{[-\eta, \eta]}(x).$$

Interestingly, the system involves a flux driven for ρ by a non-local component and for u by a local one, which makes it challenging to derive upwind type schemes. Nevertheless, central schemes as LxF, NT and KT can be directly applied.

In [10], the local existence of (4.3) has been established as well as a subcritical region for the initial data to avoid $u_x \rightarrow -\infty$, which is given by $u'_0(x) + \rho_0(x) \geq 0$, $\forall x \in \mathbb{R}$. We choose the initial data

$$\rho_0(x) = 0.2 + 0.1 \sin(\pi x), \quad u_0(x) = 0.4 + \frac{0.3 \cos(\pi x)}{\pi},$$

which fulfills the subcritical condition, to test the convergence. The final time is given by $T = 0.15$, $\eta = 0.05$, $\Delta x = \frac{1}{20} \cdot 2^{-n}$ with a reference solution computed by the KT scheme and $n = 7$. The expected convergence rate can be obtained in Table 4. To test the performance of the different numerical schemes, we consider numerically the limit $\eta \rightarrow 0$. Formally, we expect that the velocity converges to the Burger's equation (decoupled from the density). The solution of the density strongly depends on the velocity. We consider a Riemann problem in u , which results for the Burger's equation in a rarefaction wave. Formally, this creates a vacuum in the

Table 4: L^1 errors and convergence rates for the smooth initial data and the non-local Euler equations.

n	LxF		NT		KT	
	L^1 -error	c.r.	L^1 -error	c.r.	L^1 -error	c.r.
0	6.07e-02	-	1.47e-02	-	5.58e-04	-
1	3.20e-02	0.92	4.12e-03	1.83	1.62e-04	1.79
2	1.64e-02	0.96	1.15e-03	1.84	4.39e-05	1.88
3	8.33e-03	0.98	3.30e-04	1.80	1.19e-05	1.89
4	4.19e-03	0.99	9.00e-05	1.88	3.09e-06	1.94
5	2.10e-03	1.00	2.37e-05	1.93	7.80e-07	1.99

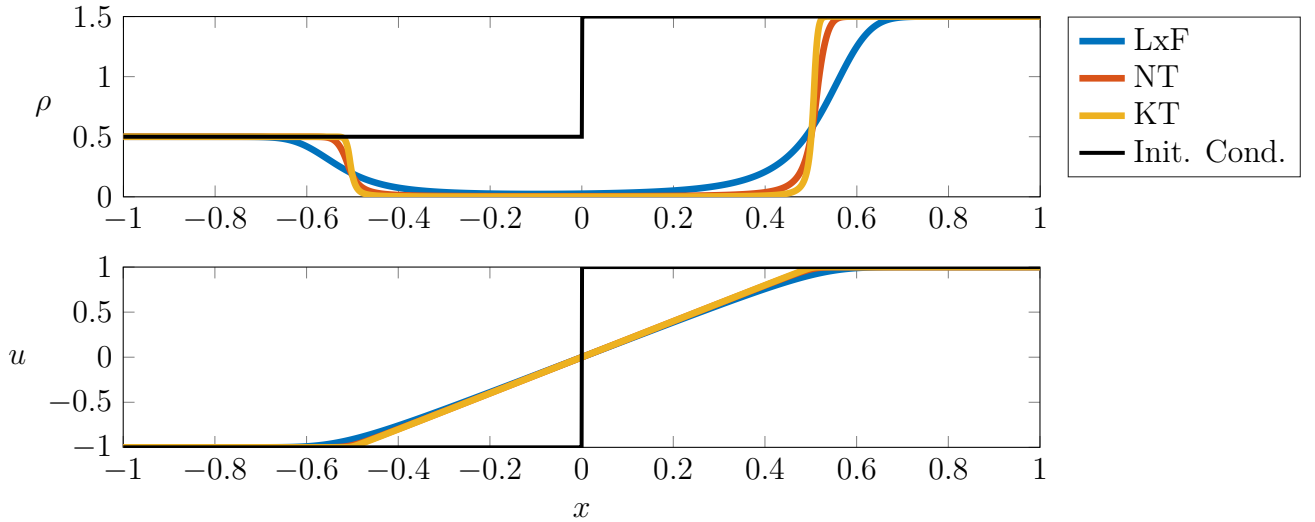


Figure 6: Numerical solutions of the non-local Euler equations at $T = 0.5$ obtained by different numerical schemes for $\eta = 2 \cdot 10^{-3}$.

density. The solutions by the different schemes at $T = 0.5$ and for $\eta = 2 \cdot 10^{-3}$, $\Delta x = 10^{-3}$

$$\rho_0(x) = \begin{cases} 0.5, & x \leq 0, \\ 1.5, & x > 0, \end{cases} \quad u_0(x) = \begin{cases} -1, & x \leq 0, \\ 1, & x > 0, \end{cases}$$

are shown in Figure 6. The numerical approximations confirm the formal results. Nevertheless, we note that to best of our knowledge the limit of $\eta \rightarrow 0$ has not been investigated yet and a further more deep analysis is necessary. In particular, the numerical evidence might be deceiving as discussed in [16].

4.4 Non-local in velocity

In (1.1) the convolution is computed between the kernel function and the state variable as a quantity of interest. Some non-local models consider different quantities, which might depend in a nonlinear fashion on the state variables. For the particular example of traffic flow models this might be the convolution of the velocity, see e.g. [13, 21, 24]. Following the strategy from Sections 2 and 3, NT and KT schemes can be derived in a similar fashion. Exemplarily we consider the non-local generalized Aw-Rascle-Zhang (GARZ) model introduced in [13]. The

modeling equations are given by

$$\begin{aligned}\partial_t \rho + \partial_x(\rho(\omega_\eta * v(\rho, \rho/q))) &= 0, \\ \partial_t q + \partial_x(q(\omega_\eta * v(\rho, \rho/q))) &= 0.\end{aligned}$$

Here, ρ is the density, q the momentum, ω_η a non-increasing kernel function with compact support on $[0, \eta]$ and unit integral, and v is a suitable velocity function.

Due to the different structure of the non-local term slight modifications are necessary to the NT and KT scheme. To approximate the non-local term in the NT scheme, we can adapt (2.10) in a straightforward manner by replacing ρ with suitable evaluations of the velocity. More modifications are necessary to approximate the temporal derivative of the non-local term, even though the computations are straightforward. In particular, we have

$$\partial_t v(\rho, q/\rho) = \partial_t \rho(v_1(\rho, q/\rho) - q/\rho^2 v_2(\rho, q/\rho)) + \partial_t q v_2(\rho, q/\rho),$$

with v_1 and v_2 the partial derivatives of v with respect to the first and second argument. Using this, we can compute $\partial_t(\omega_\eta * v(\rho, \rho/q))(t, x)$ and additionally, the temporal derivative of ρ and q can be replaced by the spatial derivative of the flux. For the NT scheme the resulting term is then approximated similar to (2.11) by using an appropriate quadrature rule and approximating the spatial derivatives by the minmod limiter. We note that the adjustments for the KT schemes are similar and need to be applied to the left and right values.

Due to the simple structure of the system we can compare the numerical results to a Godunov-type scheme, which has been considered in [13] and the LxF scheme. The velocity function is given by $v(\rho, w) = w - 6\rho$, the kernel is the linear decreasing one with $\eta = 0.1$. For the discontinuous test case we consider a jump in the momentum:

$$\rho_0(x) = 0.05, \quad q_0(x) = \begin{cases} 7/400, & \text{if } x \leq 0, \\ 1/25, & \text{if } x > 0, \end{cases}$$

with constant boundary conditions. Note that this initial condition corresponds to a jump in the so-called Lagrangian maker $w = q/\rho$ from 0.35 to 0.8. In particular, this jump remains in the analytic solution and is transported with a non-local speed. Hence, in Figure 7 we display the approximate solutions at $T = 1$ with $\Delta x = 10^{-2}$ for ρ and w . We can obtain that the jump in w is approximated most accurately by the KT scheme. For the smooth test case we consider the interval $[-1, 1]$ and

$$\rho_0(x) = 0.3 + 0.2 \sin(\pi x), \quad q_0(x) = (0.3 + 0.2 \sin(\pi x))(1.9 + 1.25 \sin(\pi x)).$$

The reference solution is computed by the KT scheme and $\Delta x = \frac{1}{20} \cdot 2^{-7}$. Similar observations as in all the previous test cases can be made. The convergence rates are displayed in the Table (5).

5 Conclusion

We considered non-staggered central approaches for systems of non-local balance laws. Based on the approach by Nessyahu and Tadmor in [39], we extended the approaches [6, 27] for scalar non-local conservation laws to systems with source term and prove upper and lower bounds on the approximate solutions. To reduce the numerical dissipation, we extended the approach by Kurganov and Tadmor [36], which has been considered for local conservation laws and splits the cells into smooth and non-smooth parts. Both schemes make use of adequate quadrature rules

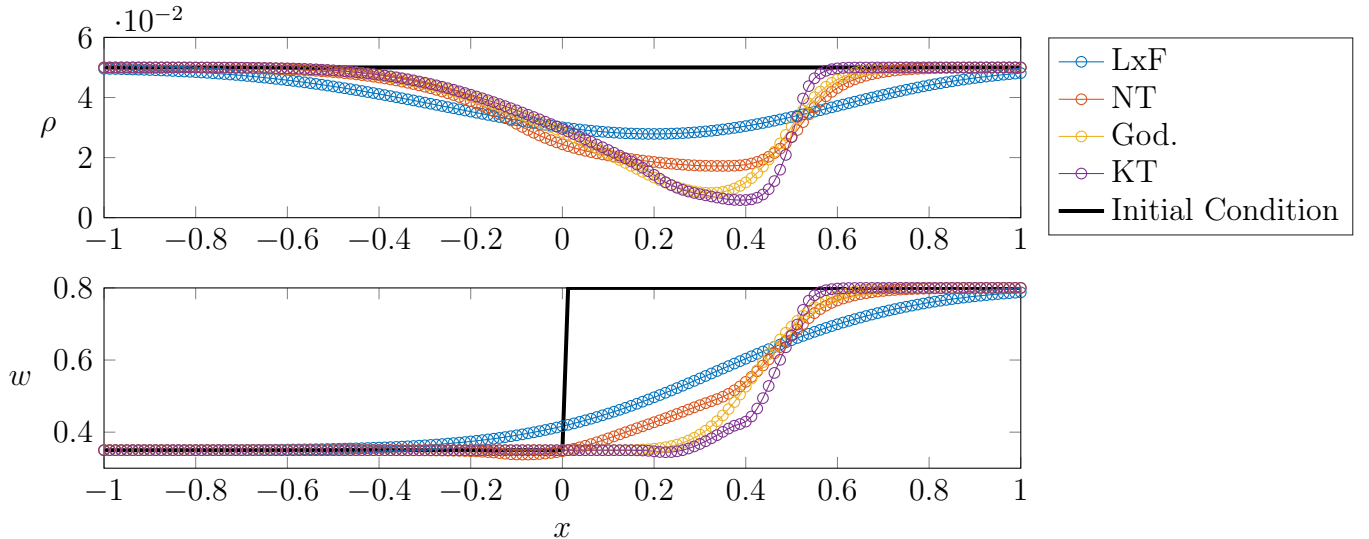


Figure 7: Numerical solutions of the non-local GARZ model at $T = 1$ obtained by different numerical schemes.

Table 5: L^1 errors and convergence rates for the smooth initial data and the non-local GARZ model.

n	LxF		NT		God		KT	
	L^1 -error	c.r.	L^1 -error	c.r.	L^1 -error	c.r.	L^1 -error	c.r.
0	5.99e-01	-	1.33e-01	-	1.37e-02	-	2.41e-03	-
1	3.67e-01	0.71	4.42e-02	1.59	6.68e-03	1.04	6.75e-04	1.84
2	2.09e-01	0.82	1.51e-02	1.55	3.29e-03	1.02	1.83e-04	1.88
3	1.12e-01	0.90	4.36e-03	1.79	1.63e-03	1.01	4.82e-05	1.93
4	5.84e-02	0.94	1.23e-03	1.82	8.13e-04	1.01	1.30e-05	1.89
5	2.98e-02	0.97	3.42e-04	1.85	4.06e-04	1.00	3.43e-06	1.92

to account for the non-locality. Their main advantage is that they can be easily applied to any system of non-local balance laws. Several numerical examples demonstrate this. Additionally, we explain how to derive these schemes to different non-local terms, which might involve a nonlinear function of the state variables.

Funding

J. F. is supported by the German Research Foundation (DFG) through SPP 2410 ‘Hyperbolic Balance Laws in Fluid Mechanics: Complexity, Scales, Randomness’ under grant FR 4850/1-1. S. R. is supported by NBHM, DAE, India (Ref. No. 02011/46/2021 NBHM(R.P.)/R & D II/14874).

Conflict of interest

The authors declare that there is no conflict of interest.

References

- [1] A. AGGARWAL, R. M. COLOMBO, AND P. GOATIN, *Nonlocal systems of conservation laws in several space dimensions*, SIAM J. Numer. Anal., 53 (2015), pp. 963–983.
- [2] A. AGGARWAL, H. HOLDEN, AND G. VAIDYA, *Well-posedness and error estimates for coupled systems of nonlocal conservation laws*, IMA Journal of Numerical Analysis, (2024), p. drad101.
- [3] D. AMADORI AND W. SHEN, *An integro-differential conservation law arising in a model of granular flow*, Journal of Hyperbolic Differential Equations, 9 (2012), pp. 105–131.
- [4] P. AMORIM, R. M. COLOMBO, AND A. TEIXEIRA, *On the numerical integration of scalar nonlocal conservation laws*, ESAIM Math. Model. Numer. Anal., 49 (2015), pp. 19–37.
- [5] A. BAYEN, J. FRIEDRICH, A. KEIMER, L. PFLUG, AND T. VEERAVALLI, *Modeling multilane traffic with moving obstacles by nonlocal balance laws*, SIAM Journal on Applied Dynamical Systems, 21 (2022), pp. 1495–1538.
- [6] S. BELKADI AND M. ATOUNTI, *Non oscillatory central schemes for general non-local traffic flow models*, International Journal of Applied Mathematics, 35 (2022), p. 515.
- [7] ———, *Unstaggered central schemes for one-dimensional nonlocal conservation laws*, International Journal of Applied Mathematics, 37 (2024), pp. 155–164.
- [8] R. BELLMAN, J. BENTSMAN, AND S. M. MEERKOV, *Vibrational control of systems with arrhenius dynamics*, Journal of mathematical analysis and applications, 91 (1983), pp. 152–191.
- [9] F. BETANCOURT, R. BÜRGER, K. H. KARLSEN, AND E. M. TORY, *On nonlocal conservation laws modelling sedimentation*, Nonlinearity, 24 (2011), pp. 855–885.
- [10] M. BHATNAGAR AND H. LIU, *Well-posedness and critical thresholds in a nonlocal euler system with relaxation*, Discrete & Continuous Dynamical Systems, (2021).
- [11] S. BLANDIN AND P. GOATIN, *Well-posedness of a conservation law with non-local flux arising in traffic flow modeling*, Numer. Math., 132 (2016), pp. 217–241.
- [12] C. CHALONS, P. GOATIN, AND L. M. VILLADA, *High-order numerical schemes for one-dimensional nonlocal conservation laws*, SIAM J. Sci. Comput., 40 (2018), pp. A288–A305.
- [13] F. A. CHIARELLO, J. FRIEDRICH, P. GOATIN, AND S. GÖTTLICH, *Micro-macro limit of a nonlocal generalized Aw-Rascle type model*, SIAM J. Appl. Math., 80 (2020), pp. 1841–1861.
- [14] F. A. CHIARELLO AND P. GOATIN, *Global entropy weak solutions for general non-local traffic flow models with anisotropic kernel*, ESAIM Math. Model. Numer. Anal., 52 (2018), pp. 163–180.
- [15] ———, *Non-local multi-class traffic flow models*, Netw. Heterog. Media, 14 (2019), pp. 371–387.
- [16] M. COLOMBO, G. CRIPPA, M. GRAFF, AND L. V. SPINOLO, *On the role of numerical viscosity in the study of the local limit of nonlocal conservation laws*, ESAIM: M2AN, 55 (2021), pp. 2705–2723.

- [17] R. M. COLOMBO, M. GARAVELLO, AND M. LÉCUREUX-MERCIER, *A class of nonlocal models for pedestrian traffic*, Math. Models Methods Appl. Sci., 22 (2012), p. 1150023.
- [18] R. M. COLOMBO, M. HERTY, AND M. MERCIER, *Control of the continuity equation with a non local flow*, ESAIM Control Optim. Calc. Var., 17 (2011), pp. 353–379.
- [19] R. M. COLOMBO AND M. LÉCUREUX-MERCIER, *Nonlocal crowd dynamics models for several populations*, Acta Mathematica Scientia, 32 (2012), pp. 177–196.
- [20] C. D’APICE, S. GÖTTLICH, M. HERTY, AND B. PICCOLI, *Modeling, simulation, and optimization of supply chains*, Society for Industrial and Applied Mathematics (SIAM), Philadelphia, PA, 2010. A continuous approach.
- [21] J. FRIEDRICH, S. GÖTTLICH, A. KEIMER, AND L. PFLUG, *Conservation laws with non-locality in density and velocity and their applicability in traffic flow modelling*, in XVI International Conference on Hyperbolic Problems: Theory, Numerics, Applications, Springer, 2022, pp. 347–357.
- [22] J. FRIEDRICH, S. GÖTTLICH, AND E. ROSSI, *Nonlocal approaches for multilane traffic models*, Commun. Math. Sci., 19 (2021), pp. 2291–2317.
- [23] J. FRIEDRICH AND O. KOLB, *Maximum principle satisfying CWENO schemes for nonlocal conservation laws*, SIAM J. Sci. Comput., 41 (2019), pp. A973–A988.
- [24] J. FRIEDRICH, O. KOLB, AND S. GÖTTLICH, *A Godunov type scheme for a class of LWR traffic flow models with non-local flux*, Netw. Heterog. Media, 13 (2018), pp. 531–547.
- [25] J. FRIEDRICH, S. SUDHA, AND S. RATHAN, *Numerical schemes for a class of nonlocal conservation laws: a general approach*, Netw. Heterog. media, 18 (2023), pp. 1335–1354.
- [26] P. GOATIN AND S. SCIALANGA, *Well-posedness and finite volume approximations of the lwr traffic flow model with non-local velocity*, Networks and Heterogeneous Media, 11 (2016), pp. 107–121.
- [27] ———, *Well-posedness and finite volume approximations of the LWR traffic flow model with non-local velocity*, Netw. Heterog. Media, 11 (2016), pp. 107–121.
- [28] S. K. GODUNOV, *A difference method for numerical calculation of discontinuous solutions of the equations of hydrodynamics*, Mat. Sb. (N.S.), 47 (89) (1959), pp. 271–306.
- [29] S. GÖTTLICH, S. HOHER, P. SCHINDLER, V. SCHLEPER, AND A. VERL, *Modeling, simulation and validation of material flow on conveyor belts*, Appl. Math. Model., 38 (2014), pp. 3295–3313.
- [30] K. HUANG AND Q. DU, *Asymptotic compatibility of a class of numerical schemes for a nonlocal traffic flow model*, SIAM Journal on Numerical Analysis, 62 (2024), pp. 1119–1144.
- [31] G.-S. JIANG, D. LEVY, C.-T. LIN, S. OSHER, AND E. TADMOR, *High-resolution nonoscillatory central schemes with nonstaggered grids for hyperbolic conservation laws*, SIAM Journal on Numerical Analysis, 35 (1998), pp. 2147–2168.
- [32] A. KEIMER AND L. PFLUG, *Existence, uniqueness and regularity results on nonlocal balance laws*, J. Differential Equations, 263 (2017), pp. 4023–4069.

- [33] A. KEIMER AND L. PFLUG, *Nonlocal balance laws – an overview over recent results*, in Handbook of Numerical Analysis, Elsevier, 2023.
- [34] A. KEIMER, L. PFLUG, AND M. SPINOLA, *Existence, uniqueness and regularity of multi-dimensional nonlocal balance laws with damping*, J. Math. Anal. Appl., 466 (2018), pp. 18–55.
- [35] A. KURGANOV AND A. POLIZZI, *Non-oscillatory central schemes for traffic flow models with arrhenius look-ahead dynamics*, Networks and heterogeneous media, 4 (2009), pp. 431–451.
- [36] A. KURGANOV AND E. TADMOR, *New high-resolution central schemes for nonlinear conservation laws and convection–diffusion equations*, Journal of computational physics, 160 (2000), pp. 241–282.
- [37] N. MANOJ AND S. K. KENETTINKARA, *Convergence of a second-order central scheme for conservation laws with discontinuous flux*, arXiv preprint arXiv:2501.04620, (2025).
- [38] N. MANOJ, G. D. VEERAPPA GOWDA, AND S. K. KENETTINKARA, *A positivity preserving second-order scheme for multi-dimensional system of non-local conservation laws*, arXiv preprint arXiv:2412.18475, (2024).
- [39] H. NESSYAHU AND E. TADMOR, *Non-oscillatory central differencing for hyperbolic conservation laws*, Journal of computational physics, 87 (1990), pp. 408–463.
- [40] A. SOPSAKIS AND M. A. KATSOULAKIS, *Stochastic modeling and simulation of traffic flow: asymmetric single exclusion process with arrhenius look-ahead dynamics*, SIAM Journal on Applied Mathematics, 66 (2006), pp. 921–944.
- [41] G. D. VEERAPPA GOWDA, S. K. KENETTINKARA, AND N. MANOJ, *Convergence of a second-order scheme for non-local conservation laws*, ESAIM: Mathematical Modelling and Numerical Analysis, 57 (2023), pp. 3439–3481.